Spring 2013

Transient gas chromatograph analysis of biomass synthesis gas produced in a lab scale gasifier

Eric S. Osgood
University of Iowa

TRANSIENT GAS CHROMATOGRAPH ANALYSIS OF BIOMASS SYNTHESIS GAS PRODUCED IN A LAB SCALE GASIFIER

by

Eric S Osgood

A thesis submitted in partial fulfillment
of the requirements for the Master of Science degree in
Mechanical Engineering
in the Graduate College of
The University of Iowa

May 2013

Thesis Supervisor: Associate Professor Albert Ratner

Graduate College
The University of Iowa
Iowa City, Iowa

CERTIFICATE OF APPROVAL

_____

MASTER'S THESIS

_____

This is to certify that the Master's thesis of

Eric S Osgood

has been approved by the Examining Committee
for the thesis requirement for the Master of Science
degree in Mechanical Engineering at
the May 2013 graduation.

Thesis Committee: _____
Albert Ratner, Thesis Supervisor

_____
H.S. Udaykumar

_____
Ching-Long Lin

I would like to dedicate this thesis to my parents. Their love, encouragement and support have given me the opportunity to pursue further education and a career of my dreams.

ACKNOWLEDGEMENTS

Firstly, I would like to thank my excellent advisor, Professor Albert Ratner, for his guidance, inspiration, support, and belief in me. He has given me many opportunities to grow as a person and student and for that he deserves my most sincere thank you. His excellent ideas and creativity have been deeply entrenched in my mind. This work would not have been possible without him.

I would like to thank the members of my thesis committee, Professor H. S. Udaykumar and Professor Ching-Long Lin. I have learned much from them through their courses and counseling. Both have been excellent guides in my education, and I only wish I had more opportunities to learn from them. They have sparked my interest in higher education and inspired me to continue learning for the greater good of society.

The members of Professor Ratner's research lab that have contributed to this work also deserve my gratitude. In particular, I express my sincere thanks to PhD student, Yunye Shi, and undergraduate student, Tejasvi Sharma for their guidance, motivation, and constant encouragement throughout our experiments and writing of this thesis. I also owe my gratitude to the rest of the Combustion Research Group at the University of Iowa including Zicheng Gong, Kelsey Kaufman, Jianan Zhang, Matthew Burkhalter, Mohsen Ghamari, and Taleb Salameh for many good times as well as their support. They were truly a wonderful group of people to work with.

Special thanks must also go out to the Oakdale Renewable Power Plant, under the supervision of Steve Kostenette, for their funding and support.

TABLE OF CONTENTS

LIST OF TABLES

LIST OF FIGURES

CHAPTER 1

INTRODUCTION AND LITERATURE REVIEW

1.1 Background and Motivation

This world is highly dependent on petroleum as an energy source, which is a limited non-renewable fuel. Finding sources of renewable energy are of paramount importance; biomass, a renewable source, is defined as a material that is derived from photosynthesis. Some of the most common forms of biomass are corn, switch grass, jatropha, miscanthus, wood, soybeans and animal waste. Biomass gasification and pyrolysis can provide a direct alternative to fossil fuel use. Fossil fuels such as coal can even be mixed with biomass to decrease coal consumption. Biomass is the only renewable resource that can produce useful carbon based liquid fuels and chemicals unlike wind or solar energy sources which can only produce electricity. Through biomass gasification, useful energy can be extracted from agricultural products as well as plastics, rubber, roofing shingles, construction waste and other carbon based materials that would otherwise be landfilled.

Biomass can be broken down into three main components: lignin, cellulose, and hemicelluloses. The lignin is a fibrous, cross linked polymeric substance that helps bond the cells together. The lignin yields more energy than the cellulose and hemicellulose when burned (Sjöström, 1993). The cellulose is the structural component of cell walls and is the most common organic compound on Earth. Hemicellulose is a polymer that is present along with cellulose in most plant cell walls. It is comprised of five different sugars in a highly branched compound. The composition of these polymers in the biomass affects the product gas composition.

Biomass gasification is a possible part of the solution to solve the world's climate and energy crisis. Global warming is an issue that will become increasingly important as the world's population increases. Since the biomass absorbs carbon dioxide (CO_2) through photosynthesis, then releases the same amount of CO_2 when it is gasified,

gasification technology has the potential to be carbon neutral. Another positive externality is that biomass and other waste products could end up in a landfill decaying and releasing methane, which is a more powerful greenhouse gas than CO_2, if they are not gasified.

Many applications of biomass gasification and pyrolysis technology are currently in use around the globe. Locally, the University of Iowa's Oakdale Combined Heat and Power Plant makes use of an experimental gasifier which burns seed corn. The University of Iowa's Main Power Plant is another example of biomass gasification which employs a fluidized bed gasifier. These two plants produce only steam and electrical energy, however biomass gasification and pyrolysis is also used to produce oils, liquids and synthesis gas. The last is what is examined in this paper. This synthesis gas can be combusted in a boiler to produce steam which turns a turbine to create heat, air conditioning, or electricity. Synthesis gas can also be used to provide mechanical power in diesel, gas and Stirling engines as well as gas turbines and fuel cells.

By employing the Fischer-Tropsch process, cleaned synthesis gas can be turned into various liquid hydrocarbons (Steen, 2008; Claeys, 2008). High temperature (1900°F) Fischer-Tropsch synthesis is used to produce olefins or alkenes. Then through the processes of oligomerization, isomerization, and hydrogenation, gasoline can be produced (Van Bibber, 2010). Low temperature Fischer-Tropsch synthesis is used to produce waxes and through an additional process of hydrocracking can produce diesel fuel (Lögdberg, 2007).

The University of Iowa contracted with Ag Bio-Power LLC to develop a biomass gasification system for the Oakdale combined heat and power plant. This system uses a downdraft biomass gasifier to gasify waste seed corn. Ag Bio-Power's system is able to gasify highly polluting materials such as plastic, tires, shingles, and rubber mixed with biomass without generating high levels of harmful emissions due to the characteristics of downdraft gasifiers. The hazardous materials must be similar in size to the seed corn. The

synthesis gas from this system is used to provide supplemental power to a 30 MW Hurst boiler used to produce steam for the Oakdale Research Campus. The Ag Bio-Power system is targeted at businesses that have a need for on-site heat or a business that generates their own waste that would need to be sent to a landfill. This gasifier can be used to replace the natural gas input to a boiler therefore reducing the energy costs.

1.2 Thesis Outline

After the fundamentals of biomass gasification are explained, the previous work done in this field is discussed in the following literature review. Chapter Two discusses the fundamentals of gas chromatography and how the gas chromatograph used in this work was calibrated. Chapter Three discusses the experimental setup used in this work in the University of Iowa's High Speed Combustion Laboratory.

Chapter Four explores the results obtained from the experiment and compares them to what other researchers have found. A basis for comparison is found in previous works done in the University of Iowa's Combustion Laboratory since their attempts were to investigate similar trends but with different measurement equipment and different biomasses. The intent is to compare the results of the present work with work done by Ulstad for temperature effects and compare against work by DeCristofaro for the effect of oxygen on synthesis gas yields. In order to determine which trends are the same and which differ this is a necessary step. This work also includes new and additional information since the effect of measuring with a gas chromatograph for time varied yields has never been done before.

Chapter Five offers various concluding remarks on the results and how they fit in with the results of similar experiments. Finally, a suggestion for future work and recommendations that may increase the global knowledge of biomass gasification and pyrolysis is presented.

1.3 Fundamentals of Biomass Gasification

To properly examine how beneficial biomass gasification is, it is necessary to look at the complete process of gasification. This process includes upstream processing, gasification, and downstream processing as shown in Figure 1.1 (Kumar, 2009). Upstream processing or preprocessing is where the biomass is prepared for gasification by reducing particle size, drying, and preparing the gasifying agents. The next step is gasification which is the most important and is where the biomass is converted into synthesis gas composed of carbon monoxide (CO), carbon dioxide (CO_2), methane (CH_4), hydrogen (H_2), water (H_2O) and other heavier hydrocarbons. The downstream processing consists of two steps, the first is gas clean-up & reforming and the second is gas utilization. Gas clean-up & reforming removes the tar and ash from the gas. The gas utilization process is where the synthesis gas is sent to a turbine, burner, fuel cell or other process. When a biomass particle is introduced into the gasifier, its drying and pyrolysis reactions occur quickly at relatively low temperatures then the remaining char is oxidized within the fuel bed to provide a heat source for the drying and pyrolysis reactions to continue for new particles. Once all these steps are closely examined, a complete cost benefit analysis can be performed for the biomass.

Biomass gasification encompasses the combustion, gasification, and pyrolysis processes. The combustion phase is an incomplete exothermic reaction where a fuel and an oxidizer, usually oxygen, react to produce heat and by-products. The by-products produced are CO_2, H_2O and trace gasses. Biomass combustion usually occurs at higher temperatures, approximately 900°C or higher (Khan, 2009). Pyrolysis is defined as the chemical decomposition of biomass in the presence of heat and little or no oxygen. Biomass pyrolysis typically occurs in the temperature range of 300-700°C (Williams, 1960). Gasification is defined as the incomplete combustion of biomass yielding CO and H_2 along with trace gasses, ash, and char. Gasification occurs between the temperatures of pyrolysis and combustion, typically between 600-1,000°C.

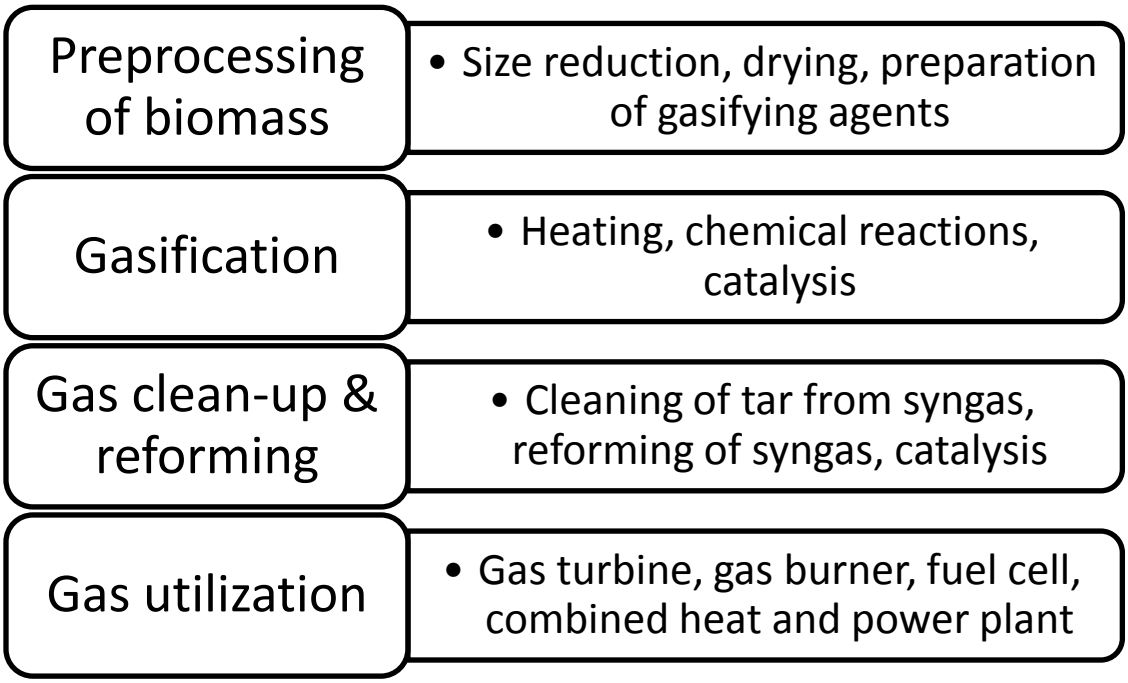

Figure 1.1. Processes involved in biomass gasification

Within the gasification and pyrolysis reaction processes there exist several smaller phases, preheating and drying, pyrolysis, and char gasification and char oxidation. The preheating and drying phase, also called dehydration, represents the loss of water from the biomass. In the overall pyrolysis phase, the majority of energy is released from the biomass. Within the pyrolysis phase there exists active and passive pyrolysis. In the active pyrolysis phase the loss of hemicellulose, cellulose and part of lignin occurs at approximately 125-500°C. In the passive pyrolysis phase the slow and continuous loss of residual lignin occurs at approximately 500°C or greater (Kumar, 2009). Within the char gasification and oxidation phase the breakdown of char occurs. This is important to gasifier performance because char must be broken down to prevent clogging and scouring of the gasifier and connected systems.

1.3.1 Types of Gasifiers

There are four main types of biomass gasifiers; they are updraft (counter-flow), downdraft (co-flow), crossdraft, and fluidized bed. They are fundamentally different in the way the air and synthesis gas flow through the system. An updraft gasifier has the air injected at the bottom while the biomass is injected at the top. The gasification products exit through the top. This is called a counter-flow gasifier because the fuel flows opposite the air. A downdraft gasifier has the air and biomass injected at the top and the products of gasification exit at the bottom. This type of gasifier is also called a co-flow gasifier because the air flows in the same direction as the biomass. A crossdraft gasifier has air passing through the fuel from side to side. A fluidized bed gasifier has heated air flow up from the bottom suspending the biomass particles which creates fluid-like behavior. Each type of gasifier has different applications, advantages, and disadvantages. Biomass with a low density should not be used in an updraft gasifier because of the high ash production associated low density biomass (Sadaka, 2008).

Gasifiers have different zones within them; the zones common to updraft, downdraft, and crossdraft gasifiers are the drying zone, the pyrolysis zone, the reduction zone, and the combustion zone. Each zone has a unique temperature and equivalence ratio with different amounts of gas concentrations. As the air or oxygen enters through the oxidation zone it begins to heat up. The exothermic reactions below the oxidation zone for a downdraft and above the oxidation zone for an updraft gasifier heat the incoming fuel and evaporate any moisture from the fuel (Lv, 2007). This zone is known as the drying zone where the temperatures typically range from 150-300°C (Lv, 2007). After the oxidizer/fuel combination is heated and dried it enters the flaming pyrolysis zone. A sharp temperature increase occurs as it enters this zone due to the governing reactions. This zone is where partial combustion occurs and the biomass releases CO_2 and

H_2O among other partial combustion species. In the experiments done by Lv et al. (2007) the steady state temperatures of their small scale gasifier were 700-900°C. In Ag Bio Power's full scale downdraft industrial gasifier the temperatures range from 1000-1300°C in the flaming pyrolysis zone (Thiessen, 2008). The next zone is called the reduction zone where tar cracking and char gasification take place. Rates of carbon conversion are slower in this zone than in those of the combustion zone due to lack of oxygen (Verhoeven, 2008). The zones are typically of different heights and sizes for different gasifier configurations. An updraft gasifier with the gasification zones labeled is shown in Figure 1.2.

Updraft gasifiers and downdraft gasifiers are quite similar in that fuel is introduced at the top of both of them. The order of the gasification zones are reversed as is the location of the gas outlet. For example, an updraft gasifier has the drying zone, pyrolysis zone, reduction zone, and oxidation or combustion zone in that order from top to bottom. The downdraft gasifier has the same zones except the air flows in a different direction. An advantage of a downdraft gasifier is that less tar is produced because the synthesis gas flows through the hottest region of the gasifier which cleans the gas as it exits (Sadaka, 2008). Figure 1.3 shows a downdraft gasifier with gasification zones labeled.

Another type of gasifier is a crossdraft gasifier. These gasifiers were designed for the use of charcoal and operate at very high temperatures, up to 1500°C (Kirubakaran, 2007). A main advantage of this type of gasifier is the very small scale at which it can operate. However, it is inefficient and the gas typically has high tar content. Because of these disadvantages cross draft gasifiers are not often used. Figure 1.4 shows a crossdraft gasifier with the gasification zones labeled.

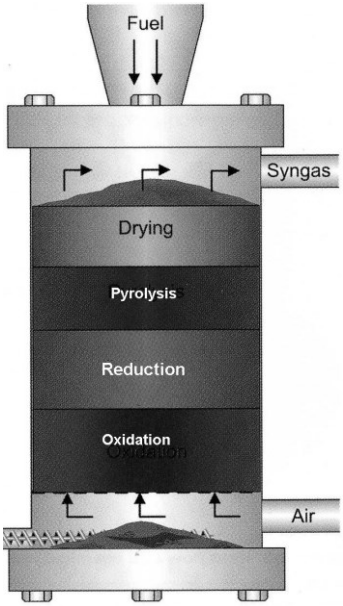

Figure 1.2. Updraft gasifier (Kneof, 2005)

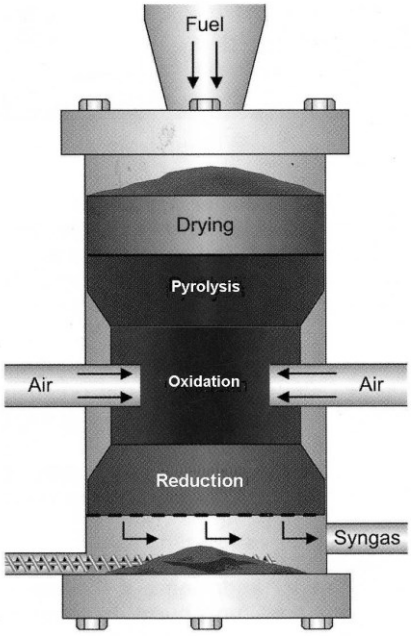

Figure 1.3. Downdraft gasifier (Kneof, 2005)

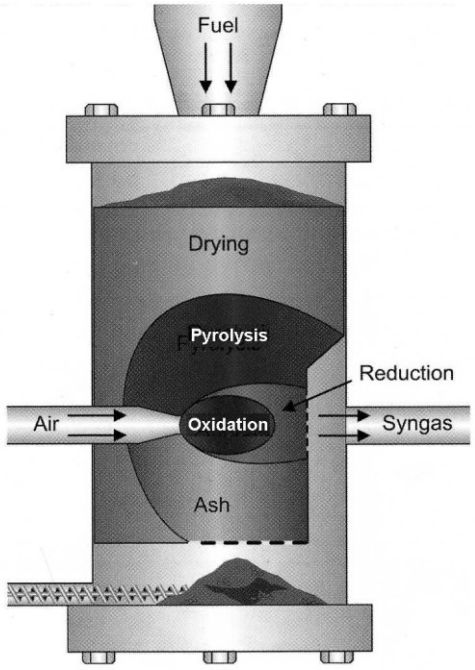

Figure 1.4. Crossdraft gasifier (Kneof, 2005)

In a fluidized bed gasifier, there exists a heated bed to transfer heat to the biomass. The bed material can either be sand, char, ash, or a combination of inert materials. The fluidizing medium is typically air, but oxygen or steam is also used. This medium must provide fluidic motion for the biomass particles. Fluidized bed gasifiers are typically used in large, industrial applications (>30 MW thermal output) such as the University of Iowa Main Power Plant. This is due to the expensive and complicated control systems they require however they have higher efficiencies (Sadaka, 2008). Fluidized bed gasifiers do not have distinct gasification and pyrolysis zones since they occur simultaneously throughout the gasifier. This enhances the heat transfer and biomass conversion efficiencies (Kumar, 2009). In fluidized bed gasifiers with inert beds, the biomass particles are subjected to intense abrasion action from the fluidized sand or other

inert bed material. This abrasive force removes much of the surface deposits such as ash from the biomass and exposes a clean reaction surface. This particle cleaning leads to a shorter residence time of several minutes instead of several hours in other gasifier types (Warnecke, 2000). Catalysts such as carbonates, limestone, calcium chloride or inorganic salts may be added. These catalysts can increase the gasifier efficiency, reduce tar production and alter synthesis gas yields (Sadaka, 2008). Figure 1.5 contains an example of a fluidized bed gasifier.

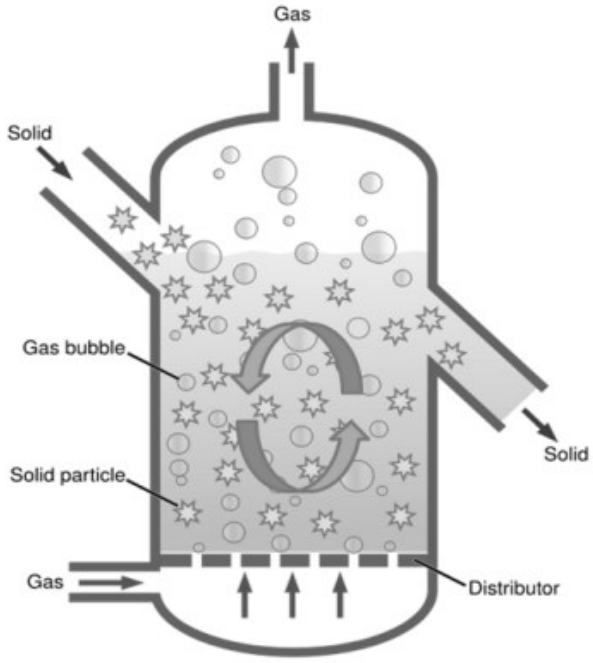

Figure 1.5. Fluidized bed gasifier (Dordt College, 2010)

The gasifier used in the Combustion Laboratory at the University of Iowa is considered a fluidized bed/updraft gasifier. Heated inert gas, nitrogen, flows up through the biomass which causes it to gasify. The gasifier at the Oakdale Combined Heat and

Power Plant is a downdraft gasifier while the gasifier at the University of Iowa Main Power Plant is a fluidized bed gasifier.

1.3.2 Gasification Reactions

The combustion equation uses a carbon-based fuel reacting with oxygen in the presence of heat to form by-products, as shown in Equation 1.1.

$$C_aH_b + O_2 \Rightarrow aCO_2 + \frac{b}{2}H_2O \tag{1.1}$$

In biomass gasification, the amount of oxygen that is present is not enough to fully combust the biomass so the resulting equation can be shown in Equation 1.2 with the biomass chemical composition in the form of $CH_xO_yN_z$ (Gautam, 2009).

$$CH_xO_yN_z + m_wH_2O + x_g(O_2 + 3.76N_2) \rightarrow$$
$$x_1CO + x_2H_2 + x_3CO_2 + x_4H_2O + x_5CH_4 + \left(\frac{z}{2} + x_g 3.76\right)N_2 \tag{1.2}$$

The highly exothermic reactions in the combustion zone are shown in Equations 1.3 and 1.4 (Kumar, 2009). These reactions are responsible for a large increase in temperature.

$$C + O_2 \rightarrow CO_2 \tag{1.3}$$

$$2H_2 + O_2 \rightarrow 2H_2O \tag{1.4}$$

As shown in Equation 1.3, the carbon and oxygen is converted to CO_2 and in Equation 1.4, H_2 and oxygen is converted into water. In these two reactions nearly all of the oxygen is consumed.

As discussed above, the next zone is the reduction zone where Equations 1.5, 1.6, and 1.7 govern (Kumar, 2009).

$$CO + H_2O \rightarrow CO_2 + H_2 \tag{1.5}$$

$$CO_2 + C \rightarrow 2CO \tag{1.6}$$

Equation 1.5 is referred to as the water gas shift reaction, which describes the amounts of H_2 and CO when H_2O is present. Equation 1.6 is known as the Boudourd reaction. Both of these are highly endothermic reactions and control the peak temperature in the reduction zone.

Another reaction is the reduction zone methane forming reaction shown in Equation 1.7 (Lv, 2007).

$$C + 2H_2 \rightarrow CH_4 \tag{1.7}$$

This reaction is also known as the Methanation reaction because it converts carbon and hydrogen into methane (Bartholomew, 1982).

Equations 1.8 and 1.9 are, respectively, the rate of steam reforming and dry reforming reactions and are more dominant at higher temperatures such as 600-800°C in the reduction zone. They also increase the CO and H_2 production while breaking down heavier hydrocarbons such as CH_4 and CO_2.

$$CH_4 + 2H_2O \rightarrow CO_2 + 4H_2 \tag{1.8}$$

$$CH_4 + H_2O \rightarrow CO + 3H_2 \quad (1.9)$$

Equation 1.9 is referred to as the methane reforming reaction (Bartholomew, 1982). Specifically, in experiments by Lv et al. (2007), the reduction zone temperature was found to be 800°C. Typically reduction zone temperatures are lower than combustion zone temperatures because the reactions in reduction zones are endothermic (Lv, 2007). When the biomass has passed through all the stages of a gasifier only the tar, ash and some char remain. This char can either be gasified again to release extraneous carbon or it can be used as a fertilizer.

1.3.3 Factors Affecting Gasification Processes

There has been a lot of research focusing on understanding the factors that affect biomass gasification. It is crucial to take the sum of the various factors in understanding the pyrolysis and gasification processes. Important factors affecting the gasification process are the amount of oxygen present, temperature, heating rate, superficial velocity, residence time, feed rate, and particle size. In this research the effect of oxygen and temperature are investigated.

1.3.3.1 Equivalence Ratio

The equivalence ratio or air-fuel equivalence ratio is directly related to the amount of oxygen present. Put simply, the equivalence ratio is the ratio of airflow to the airflow required for stoichiometric combustion. The air fuel ratio is the ratio between the mass of fuel to the mass of oxidizer in the air fuel mixture at a given time. When performing gasification experiments the equivalence ratio needs to be optimized for the particular

temperature and fuel. This number controls the reactions and products of a biomass gasifier (Reed, 2000). The equivalence ratio, λ, is given by Equation 1.10.

$$\lambda = \frac{\left(\frac{m_{fuel}}{m_{oxidizer}}\right)}{\left(\frac{m_{fuel}}{m_{oxidizer}}\right)_{stoichiometric}} \tag{1.10}$$

An equivalence ratio of 1 or nearly 1 signifies combustion as the temperature of the gasifier reaches 2000°C. A higher airflow rate results in higher temperatures which lead to higher biomass conversion rates and a higher quality of fuel. However, excessively high airflow rates result in decreased energy content of the fuel because a part of the biomass energy is spent during combustion. Higher airflow also shortens the residence time which may decrease the extent of biomass conversion (Kumar, 2009). The equivalence ratio necessary for gasification is approximately 0.25. Wang (2007) observed that with an increase in equivalence ratio from 0.16 to 0.25, the bed and freeboard temperatures increased resulting in a higher yield, higher heating value (HHV) of the gas and a higher yield of H_2 content from 8.5% to 13.9%. Increasing the equivalence ratio from 0.07 to 0.25 increased the gas yields, carbon conversion, and energy efficiencies (Kumar, 2009). It was also noted that with an increase of equivalence ratio from 0.19 to 0.27, the H_2 content varied slightly and total gas yield increased and then decreased with an optimal equivalence ratio of 0.23 (Lv, 2004). A graph of temperature versus equivalence ratio is given in Figure 1.6 (Reed, 2002).

The equivalence ratio directly affects the amount of CO, CO_2, H_2 and CH_4 produced by the gasifier. As shown in Figure 1.6, as the equivalence ratio is increased, the amount of O_2 in the system increases, and combustion occurs. A graph of mole fraction versus equivalence ratio is given by Figure 1.7 (Reed, 2002).

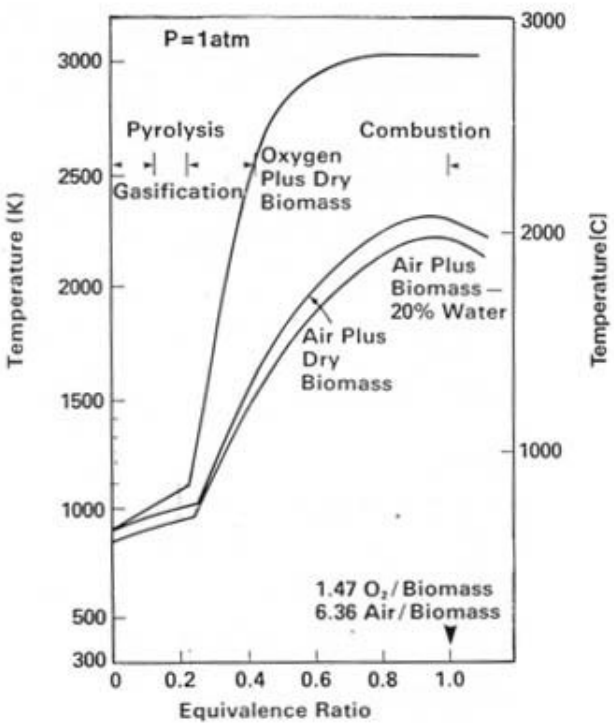

Figure 1.6. Temperature vs. equivalence ratio

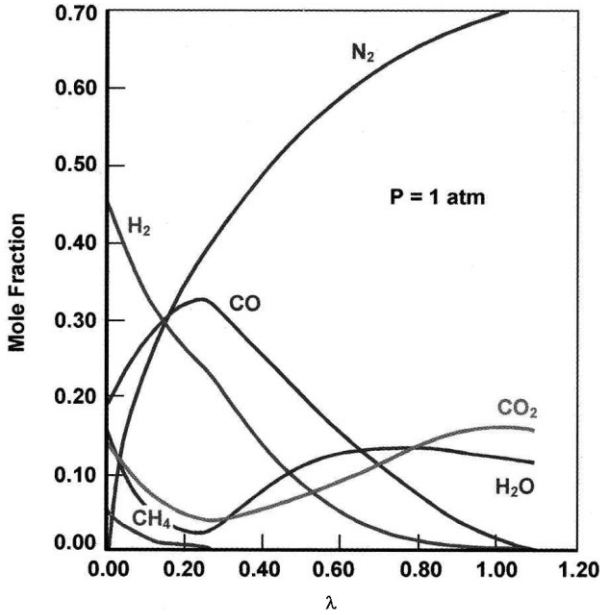

Figure 1.7. Mole fraction vs. equivalence ratio (Kneof, 2005)

As shown in Figure 1.7, increasing the equivalence ratio causes the mole fractions of CO and H_2 to decrease which is unfavorable. As the equivalence ratio increases so do the mole fractions of CO_2, N_2, and CH_4.

1.3.3.2 Temperature

The effect of temperature on biomass gasification and pyrolysis is quite large. One of the primary goals of this work is to investigate the effect of temperature on gas species evolution, specifically the evolution of CO, H_2, and CO_2 over the range of temperatures from 400-700°C. Through gas chromatography the precise species can be known at a certain point in the pyrolysis process. However, gas chromatography is not necessary to study the gas species but it is a more accurate way to detect additional permanent gasses and hydrocarbons. For example, in DeCristofaro's and Ulstad's works, also investigating temperature effects, specific sensors were used for each species. Through determination of the specific gas species an understanding of the different reactions occurring at each point in the pyrolysis is better understood.

The pyrolysis experiments performed in this work were performed at 400°C, 500°C, 600°C, and 700°C to study the trends over the temperature range. The Ag Bio-Power full scale gasifier at the Oakdale Combined Heat and Power Plant operates at temperatures between 700°C and 1300°C (Thiessen, 2008). However, through learned knowledge by operating the full scale gasifier it has reached temperatures as high as 1600°C. The stated temperature range by Thiessen is the typical range of industrial scale gasifiers.

There has been much research done on H_2 and CO production versus temperature. Kumar states that at higher temperatures there is an increase in gas yield because of higher conversion efficiency. Since the water gas shift, steam reforming, water gas, and the Boudourd reactions occur simultaneously, the concentrations of H_2, CO_2, CO, and

CH_4 in the synthesis gas are affected by temperature and partial pressures of the reactants (Kumar, 2009). The endothermic nature of the steam reforming and water gas reactions (Eqs. 1.5 & 1.8) at 750°C cause an increase in hydrogen production and a decrease in the CH_4 content. At temperatures of 850°C or higher both the steam reforming and the Boudouard reactions (Eqs. 1.5 - 1.6) dominate, resulting in an increase of CO (Kumar, 2009). In a work by Turn et al. (1998) it was found that with an increase from 750°C to 950°C, the H_2 output increased from 31% to 45% while CH_4 and CO remained fairly constant, CO_2 decreased and overall gas yield increased.

In a computational model of palm oil gasification by Lee et al. (2007), it was found that CH_4 production was greatest at temperatures between 200°C and 500°C while CO_2 production peaked at approximately 600°C. Figure 1.8 shows a normalized computer model of Lee's work.

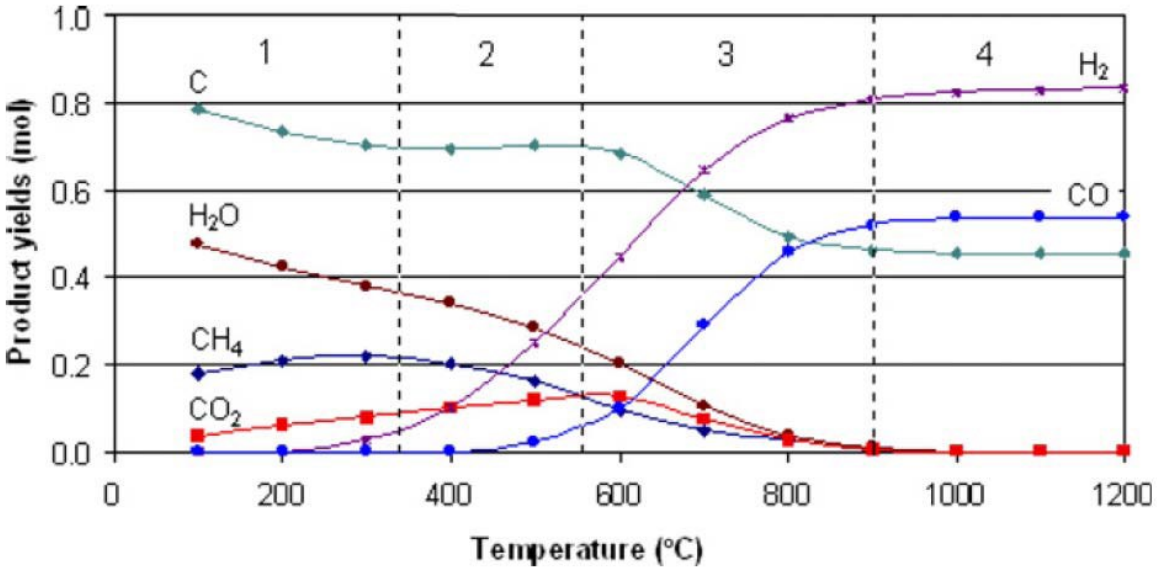

Figure 1.8. Normalized computer model results (Lee, 2007)

As shown in Figure 1.8 the yield of combustible gasses like H_2 and CO increased with temperature. At temperatures greater than 900°C, it was shown that the pyrolysis reactions were found to come to completion. The above results and trends are similar to the trends noticed in this work but an exact comparison is difficult due to the lack of experimental data and the high sensitivity of gas compositions in that range.

1.3.3.3 Superficial Gas Velocity

Another parameter that affects the gasification products is the superficial gas velocity (SGV). The SGV is directly related to the airflow rate through the gasifier and the cross sectional area of the gasifier. The SGV is a parameter that can be compared between gasifiers that are of different dimensions by normalization (Yamazaki, 2005). The SGV of a gasifier, measured in velocity, can be computed with Equation 1.4.

$$SGV = \frac{Gas\ flow\ out\ of\ gasifier}{Internal\ Cross\ Sectonal\ Area\ of\ Gasifier} \tag{1.4}$$

Decreasing the SGV has been shown to decrease tar production in fixed bed gasifiers (Devi, 2003). Specifically, decreasing the SGV from 0.7 m/s to 0.4 m/s resulted in decreasing the amount of tar (Yamazaki, 2005). According to Devi and Yamazaki, higher SGV resulted in shorter residence times and channeling which may lead to higher amounts of tar.

1.3.3.4 Other Factors Affecting Gasification Products

The size of the biomass particles greatly affects the gasifier performance. As the particle size increases the heat transfer begins to control the gasification process instead of reactions. Smaller particle size allows temperatures to be uniform throughout the

particle which may yield better synthesis gas. This uniform temperature distribution is desirable as it allows reactions instead of heat transfer to control the gasification process. Andrej Lenert used the existing laboratory setup and found that the particle size and shape were very influential factors in his pyrolysis studies (Lenert, 2008). Several other researchers found that larger particle size causes heat transfer to dominate in pyrolysis (Dupont, 2007; Kirubakaran, 2007). The goal is to have the reaction control the gasification because it promotes the highest rate of reaction and therefore the best synthesis gas (Kirubakaran, 2007).

The heating rate is another factor affecting gasification products. The heating rate is the rate at which the heat is transferred to the biomass and is measured in degrees per unit time. The heating rate used in this work is 500°C/second which is considered high. The biomass sample is dropped into a heated flow of inert gas and is assumed to come to thermal equilibrium instantaneously. The heating rate in full scale gasifiers varies and depends on several factors including but is not limited to the feed rate, moisture content of the fuel, and oxidizer flow rate.

The gas and solid residence times directly affect the products of gasification. The gas residence time is the amount of time the evolved gas is exposed to the high temperature conditions in the gasifier. This depends on equivalence ratio, superficial gas velocity, gasifier size, and biomass characteristics. The solid residence time is the length of time the biomass sample is exposed to the high temperature pyrolysis or gasification conditions in the gasifier. The gas residence time used in this work was very low at 0.2 seconds. The solid residence time used in this work was several minutes. Chen et al. (2003) conducted a parametric study on pyrolysis and gasification in a fixed bed gasifier and concluded that longer residence times and smaller particle sizes resulted in higher gas yields. Similar results were obtained in a fluidized bed reactor by Rapagnà and Latif (1997). Xu et al. (2007) also exhibited that an increase in the residence time leads to an increase in gasification efficiency in a dual fluidized bed reactor.

The fuel feed rate into the gasifier is another parameter that affects the product gas. The feed rate is measured in pounds per hour or kilograms per hour of fuel. The gasifier used in this work is a lab scale system so it uses a very small amount of fuel. The gasifier at the Oakdale Combined Heat and Power Plant consumes about 250 pounds of seed corn per hour. Increasing the feed rate too high can result in decreases in the higher heating value (HHV) and loss of efficiency (Li, 2003). The heating value of a fuel depends on the HHV and the lower heating value (LHV). LHV is based on gaseous water as a product whereas HHV is based on the products containing liquid water.

The moisture content of the air used in the gasifier will directly affect the product gas. For example, gasifying with steam has been shown to increase the H_2 content of the product gas as well as nearly doubling the value of the HHV (Pengmei, 2007). When gasifying with steam the increase in H_2 yield was accompanied by a decrease in CO yield, this can be explained by reduction zone reaction in Equation 1.3.

1.4 Biomass Characterization

Biomass is characterized as a fuel based on the following characteristics (Rajvanshi, 1986):

1. Energy content of fuel/heating value
2. Bulk density
3. Moisture content
4. Tar content
5. Dust content
6. Ash and slagging characteristics

The energy content of a fuel is expressed by how much energy will be released when it is burned. This can be expressed in terms of specific energy density. The specific energy density has units of MJ/kg or BTU/lb.

The bulk density of a biomass is defined as the mass of some amount of particles divided by the volume that those particles occupy. The bulk density of a biomass is not an intrinsic property meaning the bulk density can change based on several factors including how densely packed the biomass is. Densification of biomass is the act of compacting the biomass which increases the bulk density and removes air pockets.

The moisture content of a biomass is very important because additional energy will be required to remove the moisture from the biomass. The enthalpy of vaporization for water is very high therefore fuels with low moisture content are highly desirable. For every kilogram of water in the biomass 2,270 KJ of energy is lost due to evaporating the water. For this reason wet fuels are typically not used in biomass gasification.

Fuels that yield low levels of tar, dust, and ash are also highly desirable. Gas that contains tar, dust, and ash cannot be used in many applications until it has passed through a scrubbing process or a filter. This adds maintenance and operation costs to the gasification system. Tar buildup in the system will also increase maintenance costs.

Two other important characteristics of a biomass fuel are the ultimate and proximate analysis. An ultimate analysis reports the composition of a biomass in terms of weight percent of carbon, hydrogen, oxygen, sulfur, and nitrogen. The hydrogen determination includes that in the organic compound as well as in the water. This means that moisture is indicated as additional oxygen and hydrogen so one must be careful when using an ultimate analysis for fuels with high moisture content. A proximate analysis of a biomass gives moisture content, volatile content, and fixed carbon of a fuel during pyrolysis. With a proximate analysis, moisture is reported as grams of water per gram of dry biomass (Williams, 1996). An ultimate and proximate analysis of corn, paper sludge, and wood chips, the biomasses used in this research, is given in Chapter Three.

A biomass gasifier outputs primarily H_2, CO, and CH_4. Other gasses produced include heavier hydrocarbons, CO_2, and N_2. The combustible gas can be used in many subsequent processes and can provide many energy solutions.

1.5 Gasification Research Types

Gasification research typically focuses on one of three areas: Computational Fluid Dynamics (CFD) modeling, industrial applications, or the fundamental understanding of the gasification and pyrolysis processes. Even though research in gasification focuses on one area, they are all interrelated.

Experimental research design differs greatly depending on which specific application the research is focused on. The method and purpose of study directly affect the design of the experiment. Using CFD modeling versus industrial data versus fundamental experiments are several different methods of studying biomass gasification and pyrolysis. CFD modeling can be used to simulate a wide range of problems that would otherwise be very difficult in an experimental setup because it is simple to define boundary conditions to simplify real systems. Industrial sized systems are much larger than fundamental experimental setups and cannot localize fundamental issues. Fundamental setups cannot be made in industrial sizes or else it would be too difficult to isolate fundamental issues. Fundamental setups are not intended to generate energy but are designed to produce data. This research used a fundamental setup, which is described in great detail in Chapter Three. Since each research area is interrelated, the insight gained from this work will benefit industry and CFD modeling. Each research area is discussed in greater depth because it is important to understand how industry, CFD modeling, and fundamental research are all interrelated.

For example, a strong understanding of gasification and pyrolysis fundamentals are necessary to create accurate CFD models of a system. Validation data from industrial

sources and fundamental research experiments must also be available to validate the CFD models. Fundamental research data can provide a much better understanding of biomass reactions in each zone of an industrial gasifier, because it permits the design of a system built for specific operating conditions for industrial purposes. The current methodology is to build, test, redesign, and repeat a gasifier design which does not take into account fundamental data. CFD modeling provides highly specific information which gives insight to those working to better understand the fundamental process of gasification. Industry provides motivation and identifies real life problems that require further understanding and modeling.

The area that this work focuses on is the fundamental understanding of gasification and pyrolysis. The goal is to gain understanding and insight into the physical processes that govern gasification and pyrolysis. Specifically, this work focuses on prediction of the gas evolution from various biomasses such as corn.

Understanding of the behavior of different biomasses will give valuable insight to CFD researchers and industry. The gasses produced during this work will be analyzed with an Agilent Gas Chromatograph to understand the time evolving gasification and pyrolysis data. This work can help industry and CFD researchers advance biomass gasification and pyrolysis understanding which could yield greater energy efficiency for the world. Although the primary focus of this work is to gain a better understanding of biomass gasification and pyrolysis fundamentals, the results will be valuable to all research communities.

1.6 Thesis Objective

Much research has been conducted in the area of biomass gasification and the topic is broad. With the push for more renewable energy sources as of late, biomass gasification has become more in focus. Because of this, synthesis gas has been

implemented in boilers, heaters, and other processes around the world. The goal of this work is to contribute to the global understanding of biomass gasification and pyrolysis, specifically the effect of varying biomasses on gas species. Through an experimental study of gasifying corn, wood chips, and paper sludge, the intent is to learn which fuel yields the most potent synthesis gas at which temperature level through examination of the synthesis gas in a gas chromatograph. A gasifier's operating conditions as well as the particular biomass fuel must be optimized to obtain the desired synthesis gas composition with the least amount of impurities for the specific application. This work will help to optimize an energy producer's gasifier as well as provide more background for CFD modelers.

CHAPTER 2

GAS CHROMATOGRAPHY FUNDAMENTALS

2.1 Gas Chromatography Introduction

During biomass gasification the synthesis gas components will change as the reactions progress. Gas chromatography is a measurement method widely used in the healthcare and petroleum industries to measure the gas composition in the synthesis gas. Gas chromatography is also used to test the composition of liquids but this is not done in this work. This chapter focuses on the basic working principles and calibration of the gas chromatograph used in this work.

2.2 Gas Chromatography Principles

Gas chromatography is used to measure the chemical composition of mixtures. It is used for either liquids or gas solutions. Samples of the mixture are mixed with a carrier gas, typically helium or argon gas. This carrier gas is called the mobile phase of the gas chromatograph because it moves through the system. A gas chromatograph has several columns inside which are actually loops of tubing 10 meters in length and 0.53 mm in thickness. Inside the columns there exists an active layer which consists of a coating that absorbs and releases the components. Each component of the gas has a different absorption and release rate so the components leave the columns at different times. This is called the retention time. The columns are exposed to different temperature levels which influences the rate of release and transportation through the columns.

The gas chromatograph used in this work is a four column Agilent 490 Micro GC connected to a computer running ChemStation. However, only columns one and two were used in this work. Column one is a MS5 mol sieve and column two is a Pora PLOT U (PPU) column. Column one measures major gasses such as He, H_2, O_2, N_2, CH_4, and CO. Column two measures CO_2, C_2H_4, C_2H_6, and C_2H_2. Column one used argon as the

carrier gas and column two used helium. Figure 2.1 shows the inside of a gas chromatograph oven.

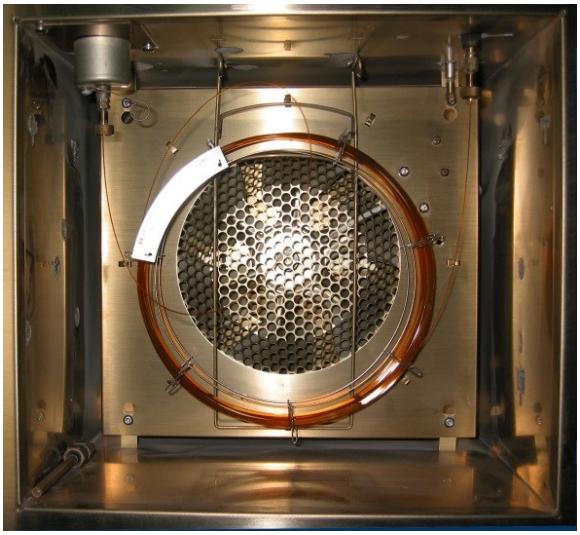

Figure 2.1. Inside of gas chromatograph oven

After the components are released from the active layer in the columns they exit one by one to flow through a detector. There are several types of detectors available for gas chromatography such as a Thermal Conductivity Detector (TCD), Flame Ionization Detector (FID), Catalytic Combustion Detector (CCD), and many more. For the permanent gasses present in this work a TCD is used. This detector identifies the thermal conductivities of the various components of the gas. The TCD contains two cells with an electrically heated filament between them, in one cell only the carrier gas, pure helium or argon, passes over the filament. While in the other cell the unknown compound with the carrier gas from the column passes over the filament. The different cells cool at different rates and the electrical resistance changes. The difference in voltage is sensed by a Wheatstone bridge which produces a large change in voltage. The voltage signal strength

depends on which gas is detected and on the concentration. The minimum concentration that is possible to measure with this detector is on the order of 100 ppm. The signal strength is linear to the concentration of the gas. When this signal is plotted in time, the peaks correspond to a certain component; this diagram is called a chromatograph. The peak area of the component is the area above the baseline. By performing integration of the peak it is possible to know the total area and therefore the amount present in the solution based on the calibration curves.

The gas chromatograph parameters for each column are shown below in Tables 2.1 and 2.2. The parameters must be the same for the calibration method as well as the testing method otherwise the retention times vary and the corresponding areas may be different leading to inaccurate results.

Table 2.1. Column one GC parameters

Column Temperature	100°C
Injection Temperature	110°C
Pressure	22.0 psi
Carrier Gas	Argon
Injection Time	40 ms
Run Time	150 sec
Invert Signal	Yes
Stabilization Time	10 sec
Sampling Time	30 sec
Sample Line Temperature	110°C

Table 2.2. Column two GC parameters

Column Temperature	60°C
Injection Temperature	110°C
Pressure	17.0 psi
Carrier Gas	Helium
Injection Time	80 ms
Run Time	150 sec
Invert Signal	No
Stabilization Time	10 sec
Sampling Time	30 sec
Sample Line Temperature	110°C

Table 2.3. Column one, MS5 (mol sieve), typical retention times

Compound	Typical Retention Time (min)
He	0.54
H_2	0.58
O_2	0.76
N_2	0.95
CH_4	1.34
CO	1.92

The carrier gas used for each column can greatly alter the retention times and results. Using helium as a carrier gas for column one is not advised because helium has nearly the same thermal conductivity as hydrogen. This makes it impossible to accurately detect the hydrogen concentration. For this reason, argon was used for column one. However, argon has almost the same thermal conductivity as carbon monoxide which may explain why the carbon monoxide peak accuracy is extremely sensitive.

When using the above parameters the expected retention times for column one and column two are tabulated in Tables 2.3 and 2.4, respectively.

Table 2.4. Column two, PPU, typical retention times

Compound	Typical Retention Time (min)
CO_2	0.76
C_2H_4	0.80
C_2H_6	0.85
C_2H_2	0.92

2.3 Calibration

The gas chromatograph had to be calibrated first to be able to do useful qualitative measurements. Calibration curves for the gas chromatograph were created with four standard calibration gasses. It is very important the same operating parameters are used for the calibration gasses as for the synthesis gas samples. From the calibration data each

specific compound's response factor was learned. The response factor is the ratio between the peak area and the concentration of a specific component.

During the calibration, a known amount of each compound was injected into the gas chromatograph which yielded a certain peak. This peak was associated with the concentration of each component in the bottle. With the response factor now known the amount of each compound present in a sample can be qualitatively determined.

Calibration gas from bottles provided by Praxair was used. Since smaller amounts of certain gasses such as CO and H_2 were expected in the synthesis gas, the calibration gas should also have small concentrations of these components. The four calibration gasses used in this work are given in Table 2.5.

Table 2.5. Calibration gas data

Calibration Gas	CO_2 [%]	CO [%]	He [%]	H_2 [%]	CH_4 [%]	O_2 [%]	N_2 [%] (balance)
1	25	10	3	4.95	2.99	0.999	53.061
2	10	15	1.99	9.98	5	2	56.03
3	15	25	1	1.98	2	3	52.02
4	0	2.02	0	0	0	0	97.98

Each calibration gas was run three times through the gas chromatograph to ensure the results were reproducible. The produced areas from the calibration gasses were related to the concentrations in the standards and a calibration curve was created. The accuracy of the calibration gas in the bottles is 1% relative. The columns of the gas

chromatograph can be cleaned of pollutants by putting the gas chromatograph into bake out mode which heats the columns up to 160°C – 180°C for an extended period of time. This allows the carrier gas to flush away pollutants. If the gas chromatograph is not put into bake out mode after testing, the calibration will need to be redone before each use. Carbon monoxide was most sensitive to not putting the gas chromatograph into bake out mode. The retention time of CO shifted to the left if gas chromatograph was not put into bake out mode. The calibration data used in this experiment is shown in Table 2.6. The amount column is the specified concentration of each component in each standard gas. The area is the integrated area calculated by ChemStation. Figure 2.2 contains the overall calibration curve produced by ChemStation with the above table of data.

Table 2.6. Calibration data

#	RT	Signal	Compound	Lvl	Amt[%]	Area	Rsp.Factor	Ref	ISTD	#
1	0.541	GC1 A	Hellium	5	1.000	20.334	4.9178e-2	No	No	
				1	1.990	40.650	4.8955e-2			
				3	3.000	63.432	4.7295e-2			
2	0.587	GC1 A	Hydrogen	5	1.980	66.804	2.9639e-2	No	No	
				3	4.950	172.350	2.8720e-2			
				1	9.980	321.360	3.1056e-2			
3	0.749	GC1 B	Carbon Dioxide	2	10.000	185.210	5.3992e-2	No	No	
				6	15.000	275.760	5.4395e-2			
				4	25.000	462.040	5.4108e-2			
4	0.769	GC1 A	Oxygen	3	9.9900e-1	3.719	2.6865e-1	No	No	
				1	2.000	7.411	2.6987e-1			
				5	3.000	10.944	2.7411e-1			
5	0.968	GC1 A	Nitrogen	5	52.020	149.510	3.4794e-1	No	No	
				3	53.061	153.580	3.4550e-1			
				1	56.030	163.350	3.4301e-1			
				7	97.980	278.810	3.5142e-1			
6	1.344	GC1 A	Methane	5	2.000	16.824	1.1888e-1	No	No	
				3	2.990	25.061	1.1931e-1			
				1	5.000	41.339	1.2095e-1			
7	1.923	GC1 A	Carbon Monoxide	7	2.020	5.604	3.6046e-1	No	No	
				3	10.000	28.053	3.5647e-1			
				1	15.000	42.550	3.5253e-1			
				5	25.000	69.458	3.5993e-1			

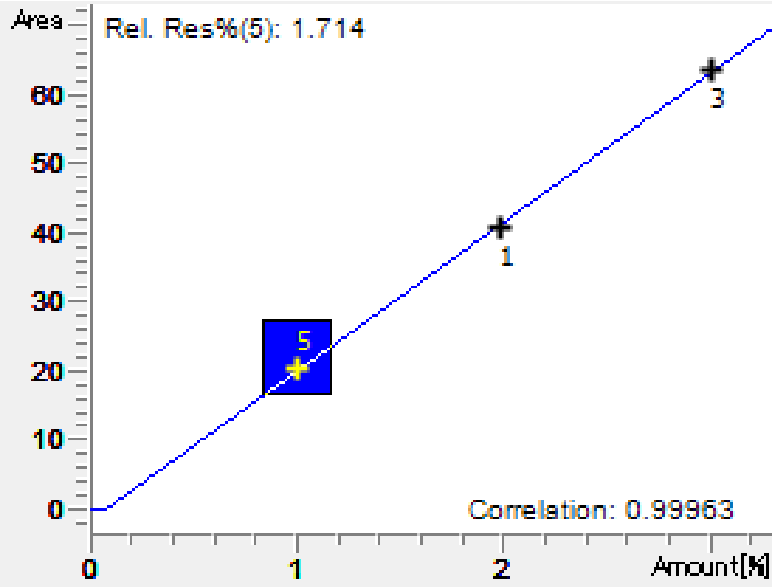

Figure 2.2. Calibration curve

The data was set to go through zero and the correlation or R-squared value for the data is 0.99963 which is very good.

The overall calibration curve is shown above but since each compound's different compound specific calibration curves are shown below in Figure 2.3. The below figures show the exact calibration curves for each compound. Shown in Table 2.7, below, are the values for each component's calibration curve. The correlation is very strong for all the components. The relationship is linear and is represented by Equation 2.1 where x represents the amount in percent and y represents the area. This equation is used by ChemStation to determine the concentration present in each synthesis gas sample.

Once the gas chromatograph was correctly calibrated the synthesis gas tests could begin. However, it is necessary to perform a gas chromatograph test of a standard calibration gas prior to a day's tests of synthesis gas to ensure the calibration table is still

valid. For best accuracy a complete calibration should be done before each experiment but this was not always possible due to time constraints.

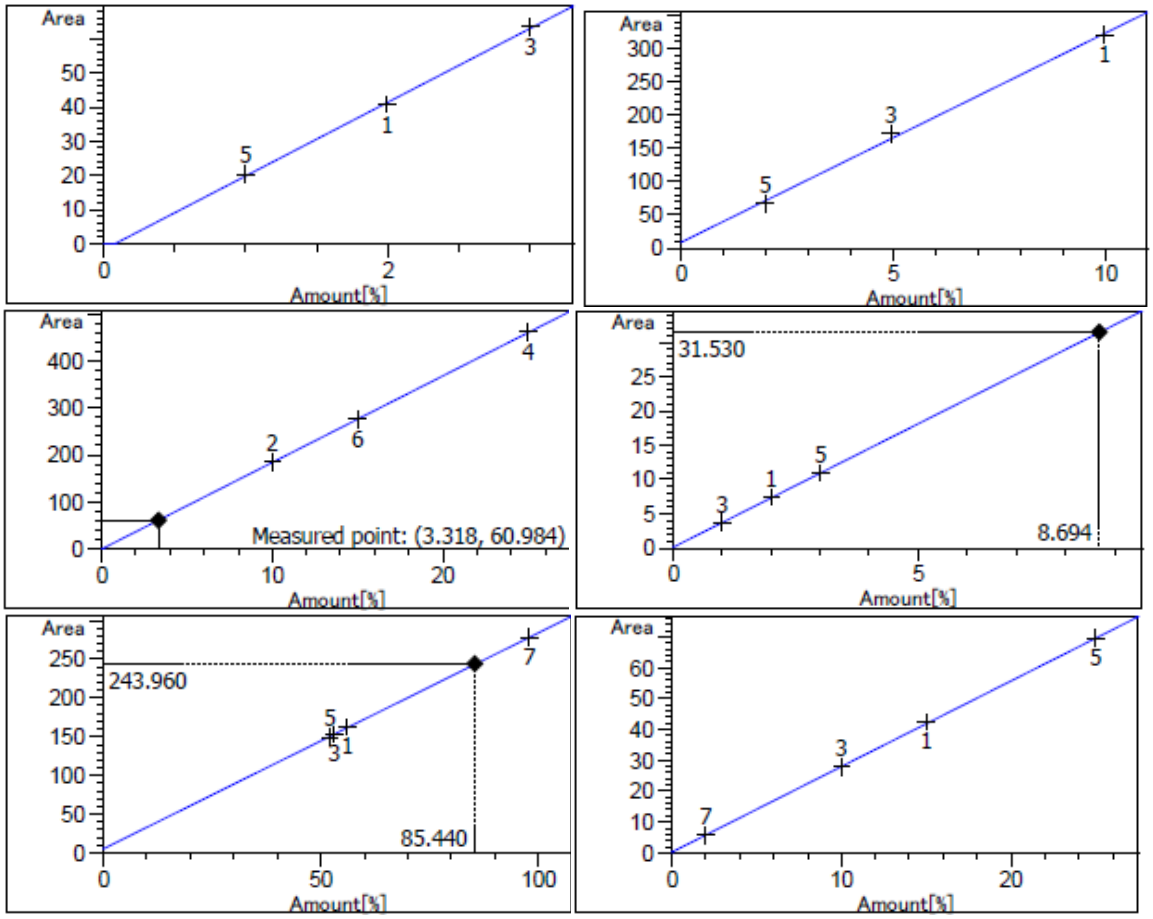

Figure 2.3. Component specific calibration curves for Helium (upper left), Hydrogen (upper right), Carbon Dioxide (middle left), Oxygen (middle right), Nitrogen (lower left), and Carbon Monoxide (lower right)

Table 2.7. Component specific linear calibration equation data

Component	m	b	Correlation
He	21.55214	-1.56058	0.99963
H_2	31.58744	8.79044	0.99878
CO_2	18.47977	-3.25032e-1	0.99998
O_2	3.61107	1.37030e-1	0.99992
N_2	2.78929	5.64189	0.99985
CO	2.78203	2.35978e-1	0.99988

$$y = mx + b \tag{2.1}$$

CHAPTER 3

EXPERIMENTAL CONFIGURATIONS AND TECHNIQUES

3.1 Materials

This work investigated seed corn, wood chips, and paper sludge. Corn is quite abundant in many Midwestern states and is already being used as a renewable energy source in ethanol production. Treated seed corn is considered toxic and must be stored under 18 inches of earth in an isolated area far from water sources (Ohio State University). The corn is considered toxic because pesticides and fungicides are applied to the corn before it is planted. Because of this reason thousands of bushels of corn are wasted every year. If these toxic additives could be removed then this unused corn could be used as a biomass fuel. Extensive research on how to remove these chemicals must be conducted before treated seed corn is a feasible energy source. However, untreated seed corn and corn stover are widely available in Iowa and the Midwest as a biomass source. Figure 3.1 shows a picture of the seed corn kernels.

The paper sludge is a byproduct of Weyerhaeuser Corp. out of Cedar Rapids, Iowa. Weyerhaeuser produces the sludge from recycling cardboard and creating cardboard pallets. They are a company focused on green manufacturing of paper related products. Paper sludge contains small strands of paper, sand, and a small amount of a plastic contaminant. Weyerhaeuser creates about 62,000 tons per year of paper sludge at 50% moisture content. Figure 3.2 shows a picture of the paper sludge.

The wood is classified as B12 fine grind wood from Wisconsin. There is an abundant supply of hard woods and soft pines around the Midwest. This wood is highly available and there is expected to be significantly more due to fungal infections and pests. The preferred use for diseased wood is gasification or burning because it completely eradicates the infections. Figure 3.3 shows a picture of the wood chips.

Figure 3.1. Corn kernels

Figure 3.2. Paper sludge

Figure 3.3. Wood chips

By understanding the chemical formulation of the materials it is much easier to predict the volatile products formed by gasification. The ultimate and proximate analysis of the materials can be seen in Table 3.1 and Table 3.2, respectively. By examining the ultimate and proximate analyses it can be predicted that higher levels of CO and CO_2 production are the result of using a fuel with higher carbon content. It can also be predicted that the majority of the permanent gasses are a result of high carbon and oxygen in the material.

Table 3.1. Material Ultimate Analysis (Ratner, 2012)

	Seed Corn	Wood	Paper sludge
Moisture	11.59%	10.60%	46.99%
Carbon	39.13%	44.32%	22.97%
Hydrogen	5.50%	5.23%	2.88%
Nitrogen	1.28%	0.08%	0.05%
Chlorine	0.04%	0.01%	0.01%
Sulfur	0.10%	0.01%	0.07%
Oxygen	41.53%	39.05%	20%
Ash	0.83%	0.71%	7.03%
Total	100%	100%	100%

Table 3.2. Material Proximate Analysis (Ratner, 2012)

	Seed Corn	Wood	Paper Sludge
Moisture	12.91%	10.60%	46.99%
Volatile Matter	74.42%	77.85%	44.99%
Fixed Carbon	7.46%	10.84%	0.99%
Ash	5.21%	0.71%	7.03%
Total	100%	100%	100%
HV [BTU/lb]	8,910	7,629	3,556

3.2 Lab Scale Experimental Setup

The experimental setup used in this work is quite similar to DeCristofaro's, Ulstad's, and Lenert's work. Many modifications and improvements have since been made. The setup which shows the main components of the system is shown in Figures 3.4 and 3.5. Figure 3.4 is a schematic of the experimental setup which shows the main components such as the industrial heater, torch system, thermocouples, flow controllers, and the gasifier. Figure 3.5 shows a picture of the experimental setup that was used for this work. Important components not seen in the schematic include particulate filter, gas chromatograph, CO sensor, and the working environment. A list of the components in their entirety can be seen in Table 3.3.

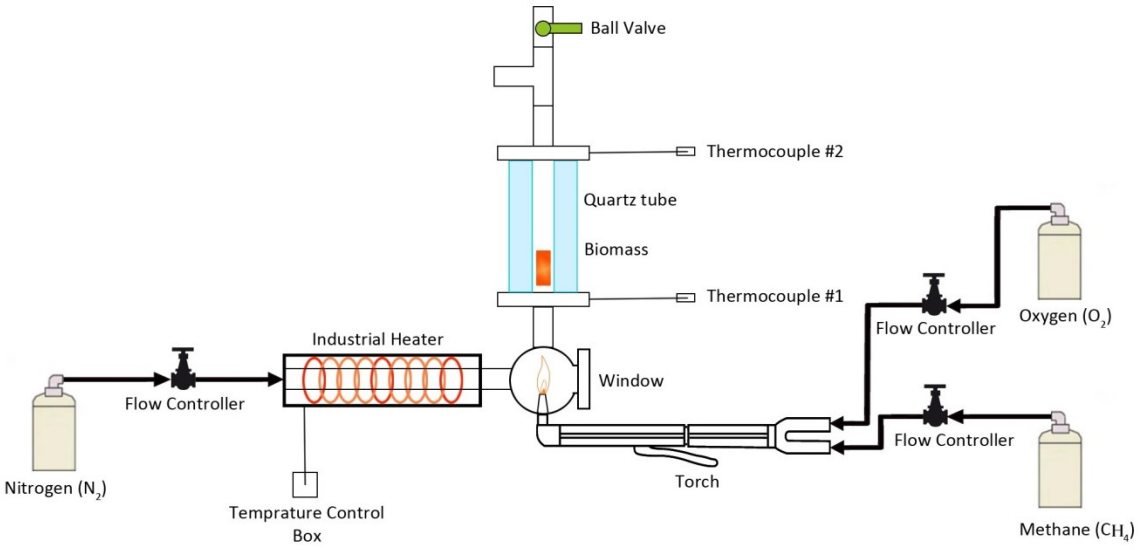

Figure 3.4. Schematic of experimental setup

The piping of the system is made from 304 stainless steel in order to resist chemical reactions and thermal cycling. The length of pipe from the heater exit to the reaction chamber is 24 cm. This piece was designed to be as short as possible to minimize heat loss. As shown in the above figure the entire length of pipe was wrapped in high temperature insulation. The vertical reaction chamber is composed of a Scientific Glass quartz tube sealed between the two titanium flanges. The quartz tube is 16.3 cm tall and has an inner diameter of one inch. The purpose of the quartz tube is to allow the experimenter to observe the reaction as it takes place. Between the lower flange and the quartz tube there is a steel mesh which allows the heated nitrogen to flow through but acts as a floor for the biomass sample. The quartz tube is held in place by a pressure fit by bolting the two flanges together. Each flange is equipped with a K-type thermocouple fit with a ferrule and nut allowing the thermocouples to be secured to the system without leaks. The bottom thermocouple is placed just below the steel mesh to accurately provide temperature data near the biomass sample. The other thermocouple is placed above the

reaction chamber to provide temperature data of the gasses leaving the reaction chamber. The two thermocouples are connected to the National Instruments USB 9219 DAQ Card which is connected to a laptop via LabView. Figure 3.6 shows a complex flow chart of the setup and most of the components including, the CO sensor, GC, computers, gas tanks, and relief valve.

Figure 3.5. Actual experimental setup

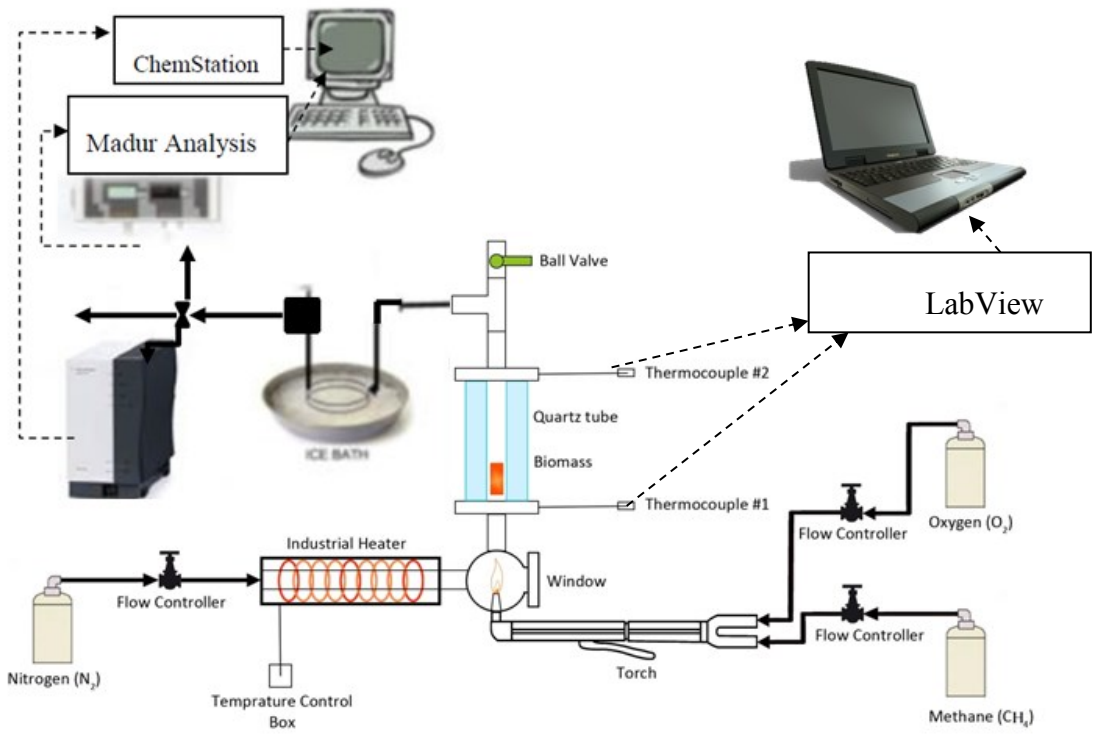

Figure 3.6. Experimental setup and flow chart

Table 3.3. Equipment list

Equipment List	
Agilent 490 Micro Gas Chromatograph	IR CO Sensor
Biomass Injection Valve	Lighter
Biomass Samples	Nitrogen Tank
Chromalox Industrial Heater	NI USB-9219 DAQ Card
Computer with LabView	Omega FMA-5400 Flow Controller
Computer with ChemStation	Omega FMA-A2409 Flow Controller
Exhaust Fan and System	Oxy-acetylene torch
Gas Chromatograph	Oxygen Tank
Gas sampling bags (10)	Particle/moisture Filter
High Precision Scale	Quartz Tube
High Tempurate Insulation	Screen Packet
Ice Bath	Stainless Steel Mesh
In-line 7 micron filter	Tubing and Fittings
	Type K Thermocouples (2)

3.2.1 CO Sensor

Since the gas chromatograph does not detect instantaneous gas release of the biomass, a CO sensor was connected in parallel to monitor the reaction. The Madur IR CO sensor was the only other sensor used besides the gas chromatograph to measure the product gas. The results from the CO sensor were initially inaccurate due to a clogged filter but after replacing the particulate filter more accurate results were achieved. The

CO sensor allowed the CO peak to be seen for each biomass sample. The range of the CO sensor was 0-10% by volume and the relative accuracy was 5.35%. The range of the CO produced in this work did not exceed 5%.

3.2.2 Gas Chromatograph

The Agilent 490 Micro gas chromatograph used in this work examined the product gas more closely and accurately. The two columns on the gas chromatograph were used to examine CO, CO_2, N_2, CH_4, and O_2. This was the first work using this setup to examine the synthesis gas with a gas chromatograph. The gas was injected into the gas chromatograph using gas sampling bags. The sampling bags introduced errors into the data because some gas may have escaped and the average of the gas evolution over the bag injection time was taken.

3.2.3 Dual Heating System

The heating system used in this work is a dual heating system because using only the industrial heater did not heat the system to the necessary temperatures. The dual heating system consists of an industrial heater, a Chromalox 9kW GCHMTI flow heater with a stainless steel body and three INCOLOY sheath elements, and a welding torch. The industrial flow heater was used to preheat the N_2 to approximately 300°C, and then the N_2 passes over the oxy acetylene torch to continue heating the flow to 400 – 700°C. Figure 3.7 contains a more specific diagram of the dual heating system. The heater was insulated with a half inch of fiberglass insulation and then wrapped in aluminum tubing. The heated nitrogen exits the heater out of a one inch NPT pipe.

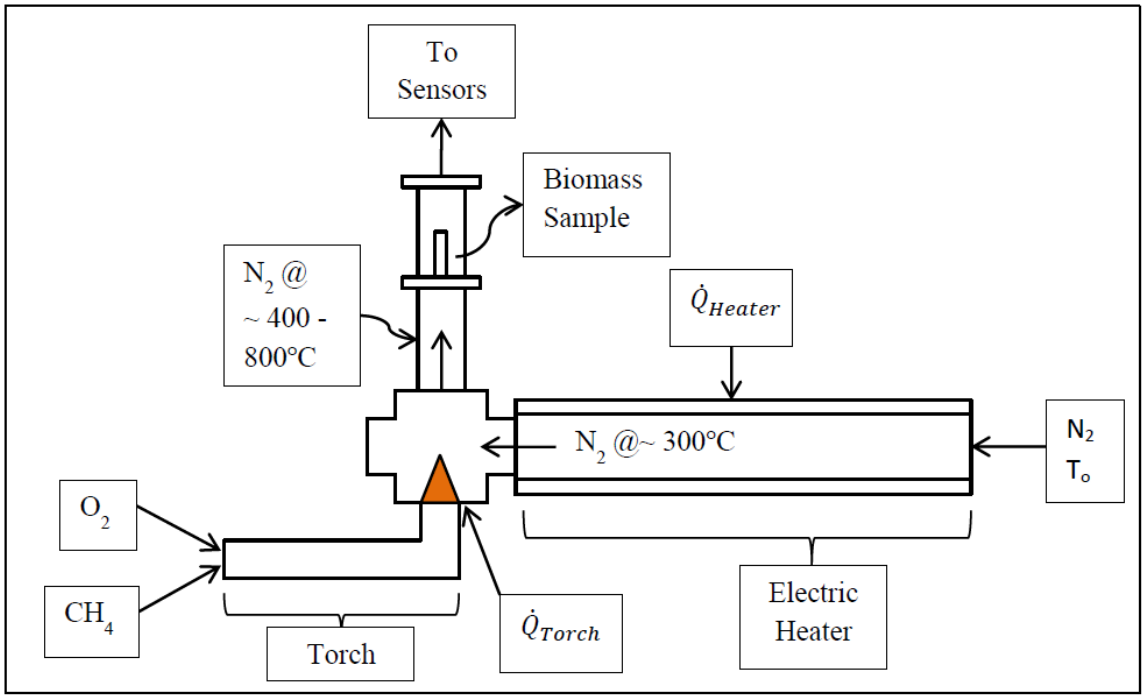

Figure 3.7. Dual heating system (Ulstad, 2010)

The version of this setup used in DeCristofaro's work experienced much difficulty with the torch frequently extinguishing. For example, when the sample was dropped into the reaction chamber the flame would extinguish due to a sharp pressure change. The flame would also extinguish when the ball valve was closed, again due to a sharp pressure change. When the char was removed between experiments the flame would also extinguish. It was initially believed the torch tip was overheating and this caused the flame instability. To remedy this, DeCristofaro cooled the torch exterior with ice during the experiments. This method did increase the flame stability and DeCristofaro was able to finish his work successfully. However, the flame stability remains an issue.

The work done by Ulstad also attempted to increase the flame stability. Several changes were made to the experiment in 2009. Firstly, it was found the setup was losing large amounts of heat due to poor insulation. To counteract the heat losses, new

insulation was added to the outside and inside walls of the pipe. High temperature insulation was wrapped on the outside of the pipe. On the inside of the pipe, a high temperature ceramic insert was used. The high temperature insulation and high temperature ceramic insert can be seen in Figure 3.8. The belief was that if the inside of the pipe maintained its temperature, the flame would not bounce off the colder walls causing flame instability. The next improvement was the addition of titanium pipe flanges. The flanges were installed at the top and bottom of the reaction chamber. The reason for the use of titanium is the lower specific heat of the titanium and the ability to withstand high temperatures. This addition helped the experiment reach and maintain the required temperatures for Ulstad's work. The most beneficial change was a new torch tip, specifically designed for methane and oxygen. These three additions by Ulstad greatly increased the reliability and stability of the torch during experiments.

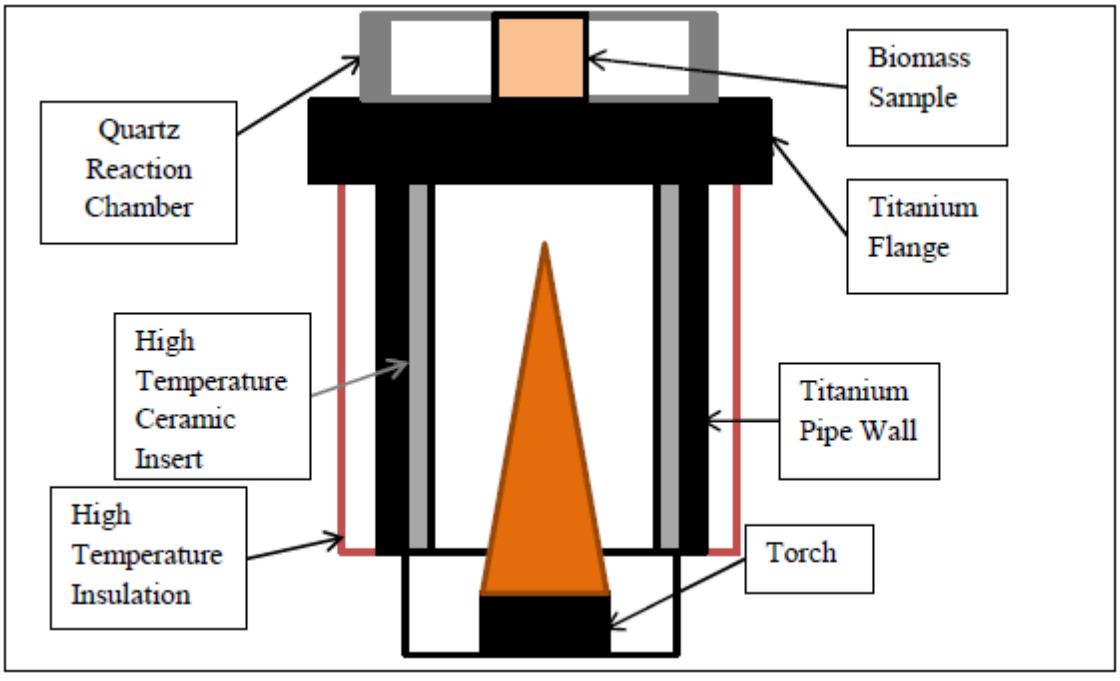

Figure 3.8. High temperature insulation and titanium pipe/flange diagram (Ulstad, 2010)

This work continued to improve the gasification system by replacing the torch tip with an identical one because some flame instability was experienced due to deformation of the torch tip. A steel collar was custom manufactured by the University of Iowa's Machine Shop to fit over the torch tip. This piece helped to reduce leaks of nitrogen and synthesis gas from the torch hole. It was hypothesized that after running the system to high temperatures the critical point of this steel collar was reached and permanent thermal expansion had caused gas to leak out of the system past the torch. To counteract this issue, the torch tip was peened and the collar was replaced and fit again over the torch tip. This helped decrease leakage. High temperature insulation was also added to the system in several places. The goal of this added insulation was to decrease the amount of time heating the system took and to reduce the amount of methane and oxygen required for running the system. Firstly, more high temperature insulation was added around the titanium pipe, this helped to decrease heat loss through this area. There was no insulation around the window which is wrapped in steel and conducted large amounts of heat away from the system so insulation was added here. There was also no insulation around the outflow end of the industrial heater and large heat losses were detected here as well. This area was also wrapped with high temperature insulation. An infrared camera was employed to identify locations losing the most heat. The system with additional high temperature insulation can be seen above in Figure 3.5. Some flame instability in this work was noted when closing the ball valve; the cause of this was pinpointed to a leak in the methane and oxygen lines to the torch. To solve this, the methane and oxygen lines were tightened and the flame instability was greatly decreased. Another issue noticed in this work was the high pressure in the reaction chamber which caused the flame to extinguish. The high pressure was found to be caused by a blockage of ash and char in the copper cooling coil. The solution to this was to remove the copper coiling coil from the system and flush it with water. Once all of these issues had been solved, the experiment ran smoothly.

3.3 Procedure

The procedure for this experiment is very important to follow mostly for safety reasons but also to maintain repeatability of experiments. A list of steps is shown below with additional details shown after:

1. Power on exhaust system
2. Check gas lines
3. Power on CO sensor and flow meters
4. Prepare ice bath for torch and sensors
5. Switch on compressed air
6. Power on electric heater
7. Set electric heater temperature to 400°C
8. Open LabView
9. Prepare biomass samples
10. Open O_2 and CH_4 tanks
11. Switch on O_2 and CH_4 lines
12. Light and insert torch when electric heater temperature is reached
13. Adjust O_2 and CH_4 flow rates for appropriate temperature
14. Once appropriate temperature is reached, switch OFF compressed air, switch on N_2 line
15. Open N_2 tank
16. Set N_2 flow rate to 40 SCFM
17. Perform experiments
18. Extinguish torch
19. Switch off O_2, CH_4, N_2 lines and tanks, turn on compressed air
20. Cool down electric heater
21. Analyze data

On the day prior to experimentation the ice baths are placed in the freezer and the gasification system is cleaned. On the day of experimentation, firstly, the gas lines are to be traced from every tank to the gasifier setup to ensure proper configuration. Then the gas chromatograph is calibrated and the exhaust system is powered on. This system is for safety and allows the gas tanks to be used only once the exhaust system is on. Approximately thirty seconds after powering on the system a loud click will be heard signifying the tank safety valves are open. If a click is not heard, the system needs to be reset by putting the switch in the off position and pressing the reset button and then restarted. The CO sensor and two flow meters should also be powered on and warmed up now.

Once the sensors are warmed up, the ice baths can be prepared. One ice bath is to cool the torch during use and the other cools the synthesis gas before it enters the CO sensor and gas chromatograph. Next the compressed air is turned on to 80 SCFM and the electric heater is powered on to 400°C. Compressed air is used to preheat the system because bottled nitrogen is more expensive. The compressed air comes from an air compressor on the roof of the Seaman's Center. A very important consideration is that the compressed air must be turned on and flowing through the electric heater before it is powered on to ensure that the INCOLOY heater elements do not overheat and melt.

The computer running LabView is powered on and the appropriate LabView setup is chosen. LabView is used to monitor the temperatures across the gasifier. Preheating with the electric heater takes about thirty minutes and in this time the biomass samples are prepared and inserted into sample baskets. Fine steel mesh is bent into a cylindrical shape for the sample baskets and a biomass sample of approximately 1 gram is inserted. The size of the basket is about 80 mm in height and 15 mm in diameter as shown in Figure 3.9. The baskets are weighed prior to filling with biomass. The baskets are weighed again with the biomass then once more after gasification. The gas sampling bags must also be evacuated at this time.

Figure 3.9. Biomass sample packet

When the system has reached the temperature set on the electric heater, the O_2 and CH_4 bottles are opened and the flow rates are set according to the desired temperature. The ratio of O_2 to CH_4 flow rates is initially set to 2.64 (Q_{O2}/Q_{CH4}) to ensure there is not much excess oxygen entering the gasifier. Next the torch is lit with a grill lighter and the nozzles are slowly opened until the flame is stable. The torch is then inserted into the torch hole of the experimental setup and held steady by a clamp and a set screw. The torch is checked frequently to ensure it has not been extinguished. If it has been extinguished, both valves must be closed and the torch is to be removed from the system and relit. The system temperature is then monitored as the experiment heats up. Setting the proper flow rates for the torch is a trial and error process where previous flow rates were used that produced a certain temperature and then the current flow rates are adjusted to reach the desired temperatures. To study the effect of oxygen on the pyrolysis process the oxygen flow rate is increased for a sample and then decreased for the next sample.

When the desired temperature is reached the compressed air can be turned off and the N_2 bottle can be opened and the flow rate set to 40 SCFM. When switching the compressed air to nitrogen, the flow through the electric heater must never stop flowing or else the heater may be damaged. The torch should also be monitored at this time.

When this step was performed by DeCristofaro the torch would become unstable and extinguish itself and release O_2 and CH_4 into the system and surroundings so a large exhaust fan is turned on during this step as a safety precaution in addition to the main exhaust system. With the current setup, torch stability is much less of an issue and it rarely extinguishes itself.

Table 3.4. Experimental parameters

Temperature	O_2/CH_4	O_2 Flow Rate (LPM)	CH_4 Flow Rate (LPM)	Excess O_2
400°C Ratio 1	2.46	3.2	1.3	2.71%
400°C Ratio 2	3.08	4.0	1.3	6.17%
400°C Ratio 3	3.46	4.5	1.3	8.63%
500°C Ratio 1	2.23	3.8	1.7	4.36%
500°C Ratio 2	2.53	4.38	1.73	6.56%
500°C Ratio 3	2.83	4.93	1.74	9.11%
600°C Ratio 1	2.13	5.8	2.72	2.72%
600°C Ratio 2	2.26	6.16	2.72	4.42%
600°C Ratio 3	2.49	6.79	2.72	6.93%
700°C Ratio 1	2.62	4.98	1.9	5.99%
700°C Ratio 2	2.99	4.4	1.47	8.16%
700°C Ratio 3	3.2	6.25	1.95	9.36%

Three experiments are performed for each temperature at a different oxygen level. The experimental parameters are defined before the experimentation begins. Table 3.4 shows some experimental parameters for the torch and the amount of oxygen present in the gasification stream.

After several minutes of N_2 flowing through the system, it will reach equilibrium and testing can begin. The exact time, material, experimenters present, O_2 and CH_4 flow rates, chamber temperature, and sample mass are recorded prior to sample insertion. When performing experiments at multiple temperatures the lowest temperature should be performed first. It is necessary to place the CO sensor in a spot where it is visible during the experiment. One gas sampling bag is filled with baseline gas to examine the exact N_2, O_2, CO_2, and CO content in the gas. The sample is then dropped into the reaction chamber through the ball valve. The upper thermocouple must be removed otherwise the sample will become stuck and will not enter the reaction chamber completely. Then the ball valve is closed and the upper thermocouple will be replaced. When the ball valve is closed there is a sharp pressure difference throughout the gasifier and the flame may become unstable and extinguished so it is necessary to pay close attention to the flame. By closing the ball valve the synthesis gas will be directed through the ice bath, silica filter, CO sensor and will then be collected into gas sampling bags. During this time the CO sensor is closely watched to monitor the gasification and pyrolysis process results. When the CO sensor starts reading increasing values it is time to begin filling the gas sampling bags. For every sample of biomass, one baseline sampling bag and five synthesis gas bags are filled to be later tested in the gas chromatograph. When the CO sensor reads zero, the ball valve can be opened and the biomass sample removed. The basket was then weighed with the char to determine the weight of char remaining. The experiment is allowed a few minutes to equilibrate before the next sample is inserted.

After all the experiments are completed, the N_2, CH_4, and O_2 tanks are turned off and the compressed air is turned on again. The torch is extinguished and removed and the

electric heater is set to room temperature. The torch is relit outside of the experiment to clear excess O_2 and CH_4 from the lines. The compressed air flow rate is set to its maximum to increase cooling of the system. When the electric heater's temperature reaches room temperature the heater and compressed air can be completely turned off. At this point the ice bath can be emptied and the exhaust system can be turned off.

3.4 Data Acquisition

Once all the tests are complete, the data is removed from the lab computers to be analyzed. The thermocouple files are created and labeled with the date everyday testing took place. These files were extracted from the computer and analyzed in Microsoft Excel. The CO sensor data is appended to a file and is analyzed in MATLAB. Both of these sensors use the computer clock to label the data points so it is not necessary to write down the times. The data from the GC needs to be examined to see if the software failed to integrate any peaks in the chromatographs. If it did fail then manual integration was necessary. This data was entered into Excel and analyzed in MATLAB.

CHAPTER 4

RESULTS AND DISCUSSION

4.1 Gas Chromatograph Results and Uncertainty

The concentration of gas species corresponds to the peak area and residence time as measured with the gas chromatograph. When the area is larger it means that more of a gas was detected, similarly, when the area is smaller it means that less of a gas was detected. The Agilent gas chromatograph used in this work produced a chromatograph for every sample that was tested. Shown in Figure 4.1, below, is the chromatograph for corn kernels at 700°C with oxygen ratio 1. Nitrogen is the largest peak because it had the highest concentration in the synthesis gas due to the gasification stream being nitrogen. The carbon monoxide peak had to be manually integrated for this sample and ChemStation identified the compound correctly. The next useful piece of information that ChemStation produced is the chromatograph report as shown in Table 4.1. This is the tabulated result of the chromatograph given in table form. This data along with all the other data points from the biomass samples were analyzed in MATLAB to better understand the effect of oxygen content and temperature on the evolving synthesis gas composition over time.

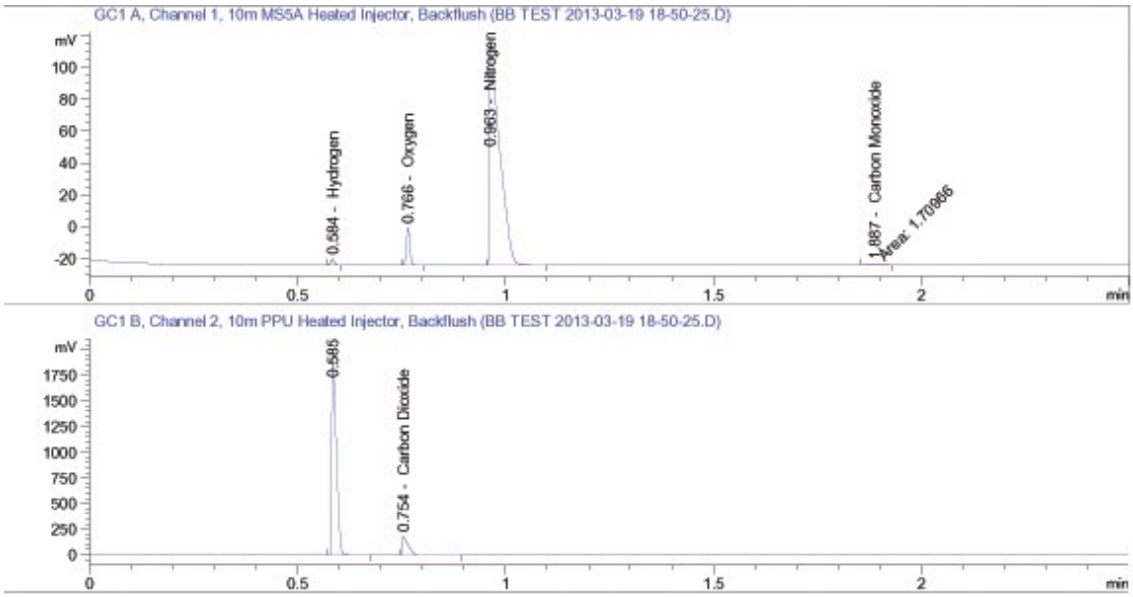

Figure 4.1. Gas chromatograph for corn at 700°C

Table 4.1. Tabulated results from gas chromatograph

Retention Time [min]	Area [mV*s]	Amount[%]	Name
0.584	2.12622	0.00	Hydrogen
0.766	12.98291	3.55736	Oxygen
0.963	240.45963	84.18544	Nitrogen
0.754	175.52032	9.51556	Carbon Monoxide

4.2 Uncertainty

Error and uncertainty entered the experiment in several different ways. Each component in the experiment introduced its own error and uncertainty. The gas chromatograph introduced a small amount of error via difference in peak area and residence time. The repeatability of the experiment is a significant factor to understand when performing experiments. It is a measure of accuracy of the gas chromatograph for each gas component. Table 4.2 contains the relative standard deviation (RSD) of area and retention time for ten samples of each gas, as stated by Agilent. According to Agilent, a relative standard deviation for area below 0.05% and a RSD for peak area below 0.1% represents excellent repeatability. This conclusion is consistent with the results obtained in this work. All the synthesis gas samples were assumed to be subject to this small amount of error.

Uncertainty was also introduced through the scale used to measure the samples. The scale was stated to be only 1% accurate. The mass flow meters have an absolute error of up to 1.5% but with repeated testing it was shown that repeatability and relative error tend to be about 1%. The thermocouples also introduced error into the system of approximately 5%. As each sensor ages the error tends to increase. The CO sensor is stated as being 5.35% accurate.

These errors affect the results in several different ways. For example, the biomass scale error affects the mass of biomass measured which later affects the length and peak of pyrolysis. The CO sensor error affects the amount of measured carbon monoxide. The error introduced by the mass flow meters may cause nitrogen dilution or increased concentration. It also affects the amount of CO_2 and O_2 introduced into the system. Human error was also introduced in that the amount of collected synthesis gas may be less than the produced amount. The errors introduced by the gas chromatograph affected

the retention time of each gas species and the peak area. The peak area is of much more interest than the retention time because it corresponds to the concentration of each gas species in the synthesis gas.

Table 4.2. Relative standard deviation of area and retention time

	Hydrogen	Oxygen	Nitrogen	Carbon dioxide
Relative standard deviation of area [%]	0.072	0.079	0.076	0.037
Relative standard deviation of retention time [%]	0.021	0.017	0.012	0.02

4.3 Excess Oxygen Volumes

Gasification rarely occurs without some O_2 present, however too much O_2 will cause the biomass to combust. To maximize CO production a small amount of excess O_2 is injected through the torch and mixed with the N_2 stream. The excess is un-combusted O_2 that did not react with the CH_4 in the torch. Ulstad found the ratio to maximize CO production for corn to be 2.64 LPM of O_2 for each LPM of CH_4. The flow rates of O_2 and CH_4 were determined experimentally by the amount of heat necessary to bring the system to the desired temperatures and by the desired amount of excess oxygen. Higher flow rates were used for higher temperatures. To determine the excess O_2 volume in the system a baseline sample was ran in the gas chromatograph for each experimental run with different flow rates and temperatures. Table 4.3 contains the excess oxygen levels tested by the gas chromatograph at different temperatures and different ratios for the

three different biomasses used in this work. It was not possible to keep the excess O_2 concentration stable for each ratio at each temperature level because of difficulty setting the flow meters. This problem was exacerbated at higher temperatures when the O_2 concentration became less diluted in the gasification stream due to increasing the CH_4 and O_2 for the torch.

Table 4.3. Excess O_2 volume per temperature range and material

	Corn	Paper	Wood
400°C Ratio 1	2.71%	2.87%	4.08%
400°C Ratio 2	6.17%	4.62%	5.13%
400°C Ratio 3	8.63%	6.68%	6.40%
500°C Ratio1	4.66%	4.66%	4.36%
500°C Ratio 2	6.36%	6.51%	6.56%
500°C Ratio 3	8.72%	9.1%	9.11%
600°C Ratio1	2.25%	2.72%	2.59%
600°C Ratio 2	4.67%	4.42%	4.42%
600°C Ratio 3	6.38%	6.96%	6.60%
700°C Ratio1	5.99%	5.50%	5.99%
700°C Ratio 2	8.16%	5.87%	8.16%
700°C Ratio 3	9.36%	8.00%	8.13%

4.4 Carbon Monoxide Evolution and Production

The CO evolution and production were determined with data from the Madur IR CO sensor. To determine the mass of CO produced for each biomass sample throughout pyrolysis as well as the total yield, Equations 4.1 and 4.2 were used (Lenert, 2008). Equation 4.1 gives the gas evolution and Equation 4.2 gives the cumulative mass produced during the pyrolysis stage where ΔT is 1 second, Q is the nitrogen flow rate [L/s], γ_{gas} is the concentration of the target gas, R is the universal gas constant [L-atm/mol-k], P_{atm} is the atmospheric pressure [atm], M_w is the molar weight of the target gas [g/mol], and T_{amb} is the ambient temperature [K].

$$m(t) = \frac{M_W \gamma_{gas} P_{atm} Q \Delta T}{R T_{amb}} \tag{4.1}$$

$$m(t) = \sum_0^{n=t} \frac{M_W \gamma_{gas} P_{atm} Q \Delta T}{R T_{amb}} \tag{4.2}$$

Using the above equations, the mass of CO was determined from the gas concentrations as measured by the CO sensor. The gas evolution for CO can be seen in Figure 4.2 for all of the tested materials. These figures contain data with the same or similar oxygen contents at a value of approximately 6% excess.

Each biomass material was gasified at 400°C, 500°C, 600°C, and 700°C. The temperature used in these plots is the gasifier bed temperature. For all of the materials, the pyrolysis temperature is generally inversely related to the pyrolysis duration. The pyrolysis duration is when the majority of the volatile gasses are released and ends when the gas evolution is negligible or when the CO sensor read 0.02% or less. It was found that as pyrolysis temperature increases the production rate of CO also increased which is in agreement with other studies. All materials yielded higher CO peaks at higher temperatures, as expected. An increase in gas evolution was present at 700°C for corn and

wood chips. This may be due to Equation 1.9 or the dry reforming reaction in the reduction zone which occurs at 600-800°C. The largest gas evolution was measured for wood chips at 700°C. Pyrolysis occurred slower at lower temperatures for all materials, with the slowest pyrolysis time for corn. This is likely due to the small exposed surface area of the corn kernels to the heated gasification stream (N_2). The double peaks seen in the figures are most likely due to different reactions dominating at different times and different local temperature levels. From Figure 4.2 it can be seen that wood chips reached the highest CO evolution, however paper sludge reached its peak in a shorter amount of time than the other materials.

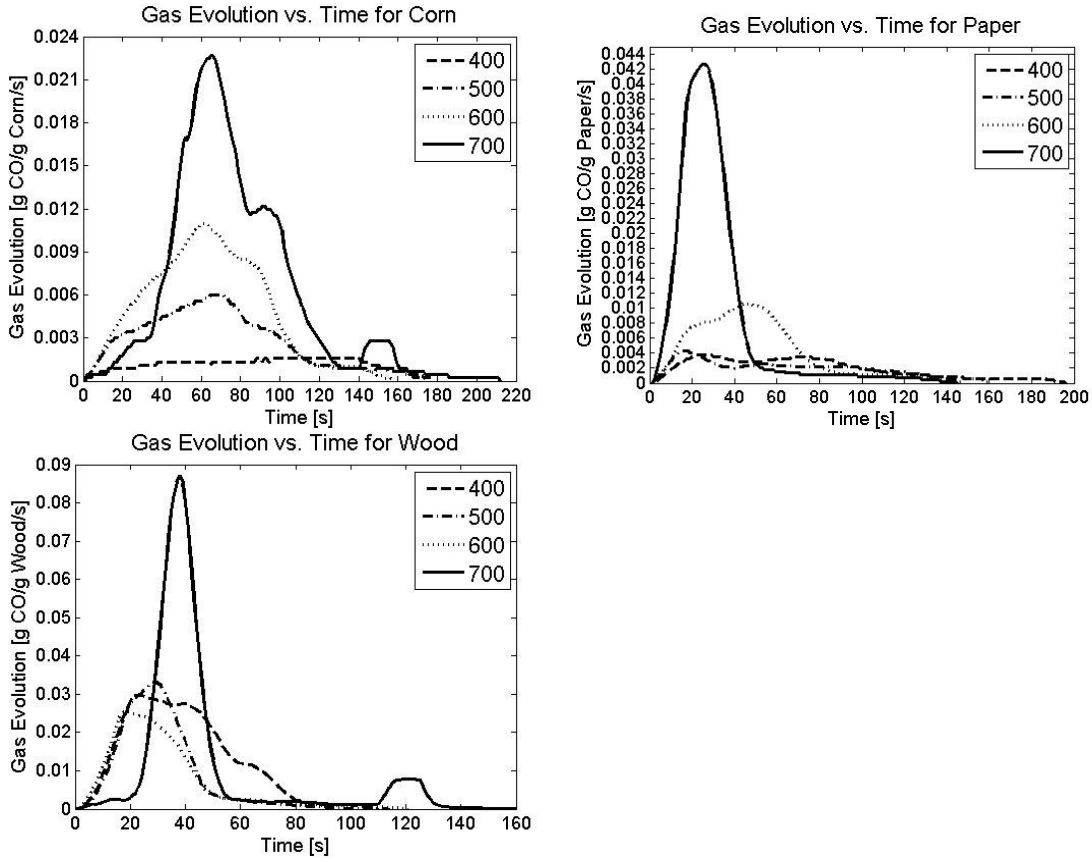

Figure 4.2. CO gas evolution vs. time for Corn (upper left), Paper (upper right), and wood (bottom) from CO sensor

Table 4.4. Approximate time to pyrolysis peak (in seconds) by material and temperature series

	Corn	Paper	Wood
400°C	106	24	30
500°C	68	17	27
600°C	62	51	31
700°C	64	25	38

From Table 4.4 it can be seen that higher temperatures positively influenced pyrolysis peaks and this trend was similar for all biomass materials examined. At higher temperatures the time to pyrolysis peak decreased while the rate of CO production increased. This signifies that the CO production equations are dominating at higher temperatures. Corn's CO yield peak was found to be the most sensitive to temperature as it took 106 seconds at 400°C to reach a peak of 0.07%. This could be due to the higher density of corn, the size of the corn kernel and the smaller surface area exposed to the heated gasification agent. The particle size of the wood chips and paper sludge was significantly smaller and their density was much higher. Wood chips were found to produce the highest amount of CO at 4.49% after 38 seconds.

The data from the CO sensor was compared to the CO data from the gas chromatograph with corn at 400°C, 500°C, 600°C, and 700°C. The CO data from the GC must be above a certain threshold or else ChemStation will not recognize the peak on the chromatograph as a compound. The area under the curve must be greater than one for

ChemStation to recognize it. If the area was larger than one but still relatively small then the concentration of CO had to be manually interpolated. Figure 4.3 contains the plots of CO evolution for corn kernels, paper sludge, and wood chips from the gas chromatograph.

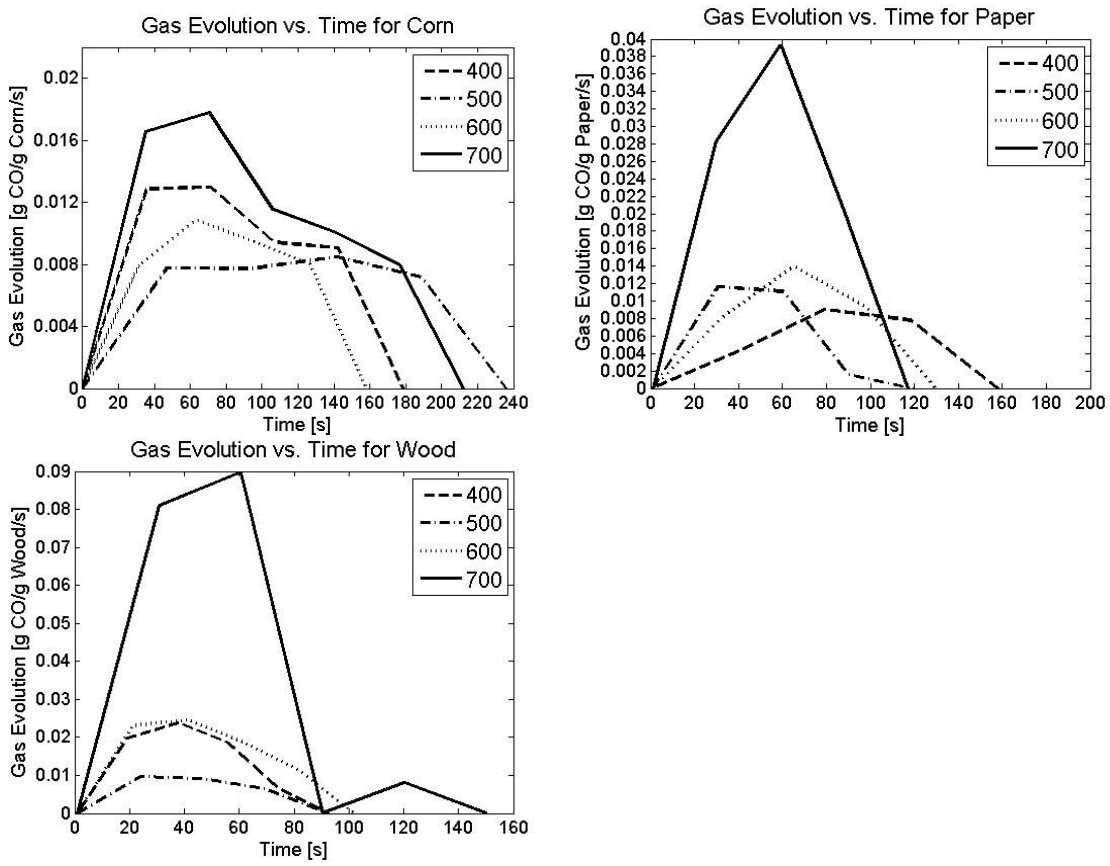

Figure 4.3. CO evolution vs. time for corn, paper, wood from gas chromatograph data

Upon inspection of this figure it can be seen that the data follows the same trends as the data from the CO sensor however the peaks are not as sharp because of the sampling method used. The sampling method used in this work time averaged the

contents of each bag. Each bag was filled for approximately ten seconds and the gas chromatograph measured the average concentration of each bag. The peak for corn in Figure 4.2 occurred at 700°C at a value of approximately 0.023 [g CO/ g Corn/s] whereas the peak for corn in Figure 4.3 also occurred at 700°C but with a value of approximately 0.018 [g CO/ g Corn/s]. This represents a percent difference of -21.7%. Corn was also found to have the longest pyrolysis time over all temperatures, which is consistent with the data from the CO sensor. This figure also shows another trend, with increasing temperature, the gas evolution increases. Due to the relative increased surface area of wood chips and the high amount of carbon contained in them, wood chips produced the greatest amount of evolved CO, as shown in Figure 4.3. A double peak was present in the CO sensor data that was also detected with the gas chromatograph in wood chips at 700°C, also shown in Figure 4.3. This double peak is likely due to char gasification reactions taking place after the initial pyrolysis has finished. This reaction was only present at 700°C because char gasification occurs only at higher temperatures. Furthermore, this figure increases the validity of the data from the CO sensor.

It was useful to examine the cumulative production of all materials. This was done by integrating each temperature series throughout the pyrolysis process and the data is plotted in Figure 4.4. These figures contain data with similar oxygen concentrations; the oxygen concentration in these figures is approximately 6% excess. As expected, wood chips at 700°C produced the highest total yield of CO. Paper sludge yielded the lowest amount of CO when compared to wood chips and corn kernels across all temperature levels. This could be due to the specific sample of paper sludge having had higher moisture content than the others or the pyrolysis may have occurred too quickly for the CO sensor to detect the entire amount of instantaneous CO produced. This factor can be controlled by performing additional experiments for each operating parameter. The heat transfer rate at higher temperatures also becomes a more significant factor. For all materials, higher temperatures resulted in significantly higher total CO yields.

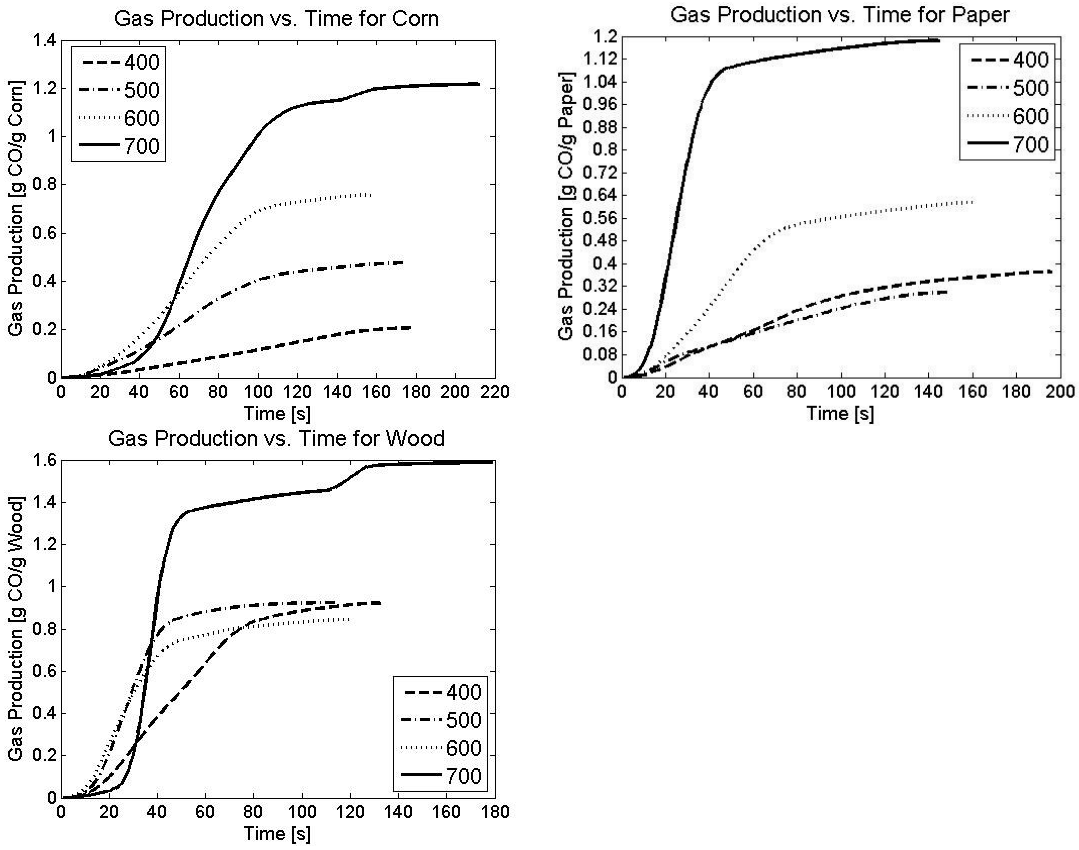

Figure 4.4. Total CO gas production vs. time for corn (upper left), paper (upper right), and wood (bottom) from CO sensor

4.5 Carbon Dioxide Concentration

The CO_2 gas evolution was determined using the gas chromatograph with synthesis gas samples being taken at several points throughout the pyrolysis stage. It was determined at each point by subtracting the baseline value from that point's value to correct for additions by the torch, as shown in Equation 4.3. At higher temperatures when

more CH_4 and O_2 are flowing through the torch, there was a greater amount of CO_2 in the baseline because of combustion of the torch reactants.

$$Percent\ Produced = Percent_{sample} - Percent_{baseline} \quad (4.3)$$

This method was performed for each material at each temperature level to understand the effect of temperature on CO_2 concentration. Figure 4.5 contains the CO_2 gas concentration versus time for corn kernels, paper sludge and wood chips. These figures contain data with the same or similar oxygen contents; the oxygen concentration in these figures is approximately 5.5% excess.

As seen in the below figure, increasing temperature has a large effect on CO_2 production for all materials. At the lower temperatures such as 400°C, 500°C, and 600°C, for all materials, the concentration of CO_2 was quite low, at approximately 1% at its peak. Yet, a surprising increase for all materials at 700°C was noticed. This could be due to the highly exothermic Equations 1.3 and 1.5, in the combustion zone and in the reduction zone, respectively. Equation 1.8, known as the rate of steam reforming equation, is also believed to play a large role in this increase of CO_2 because it is dominant in the reduction zone at temperatures in the range of 600-800C. Corn reached its peak CO_2 production slower than wood chips and paper sludge. This is likely due to the small surface area of corn exposed to the gasification stream. These figures lack smooth curves because each sampling bag represents a time averaged concentration. If an instantaneous CO_2 sensor had been used the result would look similar to Figure 4.2. Future work should be to ensure that more gas sampling bags are used to ensure that a broader set of data is produced.

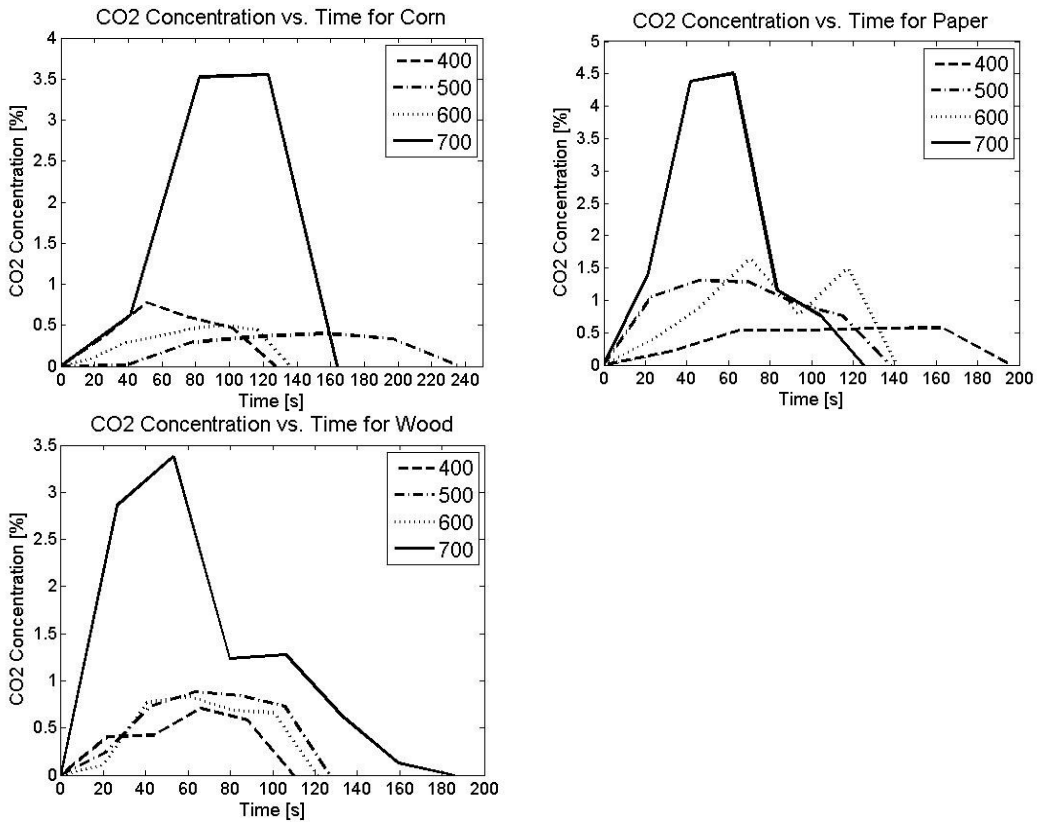

Figure 4.5. CO_2 gas concentration vs. time for corn (upper left), paper (upper right), and wood chips (bottom)

4.6 Hydrogen and Methane Concentrations

Hydrogen was measured for every experimental case however the amount detected was so small it may be considered negligible. This experimental setup had a very short gas residence time of approximately 0.2 seconds and this is why hydrogen was detected infrequently. Many industrial systems have gas residence times that are significantly longer (Kumar, 2009; Thiessen, 2008). Longer gas residence times allow the heavier hydrocarbons to be broken down into their simplest forms such as C, H_2, and O_2. This was an expected result of this experimental study. The highest amount of H_2

detected was a value of 0.48% for wood chips at 700°C with excess oxygen of 8.16%. Typically, when H_2 was detected at other times it was 0.1% or less.

Methane production was also negligible and was not present on any chromatographs produced in this work. To ensure no methane was missed the gas chromatograph was calibrated properly with methane but no methane was detected during experimentation. The lack of methane in the synthesis gas may be due to methane reforming into other compounds in the presence of O_2 and heat. The short residence time of this system also played a role in the lack of methane detected.

4.7 Water Concentration in Synthesis Gas

Water is always a byproduct of combustion and gasification. However, the water was removed in this work by the silica filter because of the risk of damaging the gas chromatograph. In this work, the torch produced excess H_2O and the gasification of biomass also produced H_2O due to the presence of water in the biomass. It was estimated that the water in the biomass weighs 20-30% of the total product weight. Although some biomasses such as paper sludge contain more H_2O than others. This mass was unaccounted for in this work.

4.8 Oxygen Concentration in Pyrolysis

As previously discussed, the presence of oxygen in the heated nitrogen stream greatly affects the pyrolysis yields. This excess O_2 reacts with the biomass during the decomposition and mixes with the C and H_2 to form CO, CO_2, and H_2O as shown in Equations 1.2-1.4. These compounds are then broken down again through heating to release the O_2 stored within the various biomass materials. The exact composition of the biomass materials can be seen in Table 3.1 above. Figure 4.6 contains the plots of O_2 concentration for each biomass material. The excess oxygen provided by the torch for

corn is 6%, for paper sludge it is 4.5%, and for wood chips it is 6.5%. It was attempted to keep the excess oxygen concentration as constant as possible of those experiments in order to only understand the effect of temperature. The amount of O_2 present in each gas sampling bag is subtracted from the baseline as shown in Equation 4.3 to show O_2 production, represented by positive concentrations, and O_2 consumption from reactions, represented by negative concentrations. Initially, the value of O_2 is 0% for all the experimental cases because that is the baseline case but this value actually corresponds to an excess concentration listed above. Common trends at 400°C, 500°C, and 600°C show an increase or much less of a decrease in O_2 consumption when compared to the 700°C cases. This may be due to a pressure wave in the system due to closing the ball valve or dropping the biomass into the chamber. Or it may be due to the initial decompositions of biomass that release O_2 before the excess O_2 reacts with other gasses to form different compounds. These reactions may have been present at 700°C but occurred too quickly to capture the increase in O_2 in the gas sampling bags. However, every material at every temperature showed the same overall dip in O_2 concentration which is associated with the reaction of O_2, C, and H_2 to form CO, CO_2, and H_2O.

The most negative concentrations of O_2 were found for wood chips at 700°C where the lowest amount was nearly -6% which was approximately twice as low as corn and paper at 700°C. The wood chips also produced the most CO and second most CO_2 at 700°C. Corn kernels consumed the least O_2 at lower temperatures whereas wood chips and paper sludge consumed the most over the lower temperature ranges. This may be due to the particle size of the wood chips as they were much smaller than the corn and had more surface area exposed. Another interesting trend is that the lowest point of each temperature series in Figure 4.6 corresponds to the peak production of CO and CO_2 as shown in Figures 4.2 and 4.5. This shows that the O_2 is being reformed into other compounds more frequently at higher temperatures. The consumption of O_2 is directly related to increasing temperature.

Figure 4.7 contains the overall gas species evolution for corn at 700°C with excess oxygen of 6%. As expected, as oxygen levels decrease the CO and CO_2 levels increase. For this particular sample CO_2 reached a concentration of nearly 10% while CO peaked at approximately 1%. These trends were consistent with other samples.

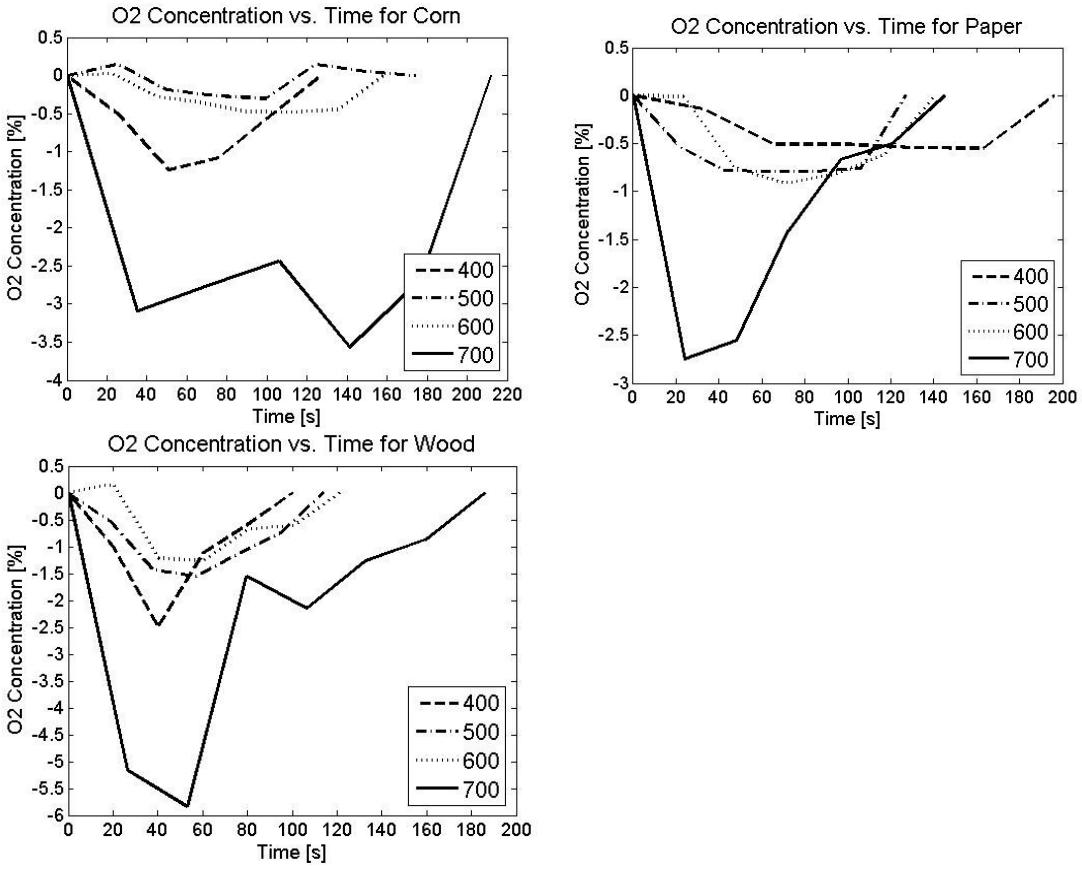

Figure 4.6. O_2 concentration vs. time for corn (upper left), paper sludge (upper right), and wood (bottom)

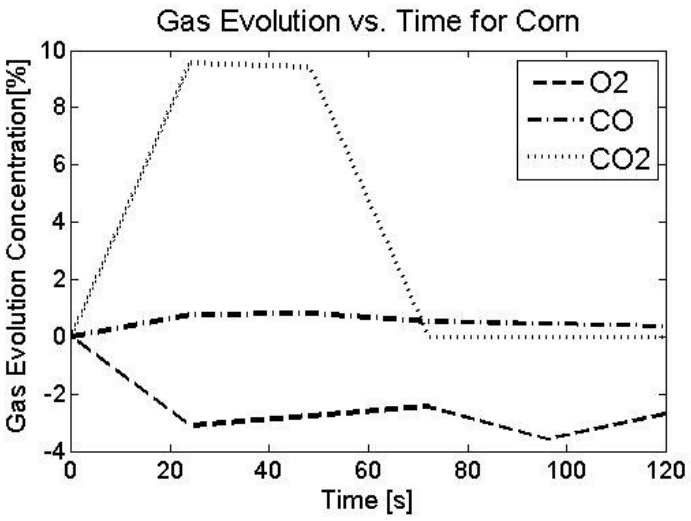

Figure 4.7. Overall gas evolution for corn at 700°C

4.9 Mass Balance

After the sample was gasified its char was weighed when available. Several corn and all the paper and wood chip samples blew away when the basket was being extracted from the system. The samples blew away because it was not advised to turn the flowing nitrogen off while the heater is hot. Measuring the weight was only possible for several corn samples due to the low char and ash density of paper and wood chips. Therefore a mass balance was only performed for several corn samples. Typically the amount of char remaining was 10-20% by weight of the beginning mass of corn, which is consistent with DeCristofaro's char weight measurements. The mass balance could be estimated for other materials using this estimate of char. To compute the mass of each component of the gasification product Equation 4.1 was used. To determine the mass balance Equation 4.4, shown below was used.

$$Total\ mass\ of\ sample = Mass_{CO} + Mass_{CO_2} + Mass_{O_2} + Mass_{char} \qquad (4.4)$$

A mass balance was computed for corn with an initial mass of 1.14 grams gasified at 500°C with excess oxygen in the gasification stream of 6.35%. Table 4.5, below, shows the mass of CO, mass of CO_2, mass of O_2 and the mass of char.

Table 4.5. Mass balance for corn at 500°C

CO [g]	CO_2 [g]	O_2 [g]	Char [g]	Total [g]
0.89	0.483	-0.504	0.22	1.09

The mass balance yielded 1.09 grams after gasification while the initial value was 1.14 grams. This results in a percent error of -4.39% which is very low. The mass balance could be repeated for other experiments but is not, due to time constraints. The oxygen mass is a negative number because the gasification process consumes oxygen during its reactions. This is due to the oxygen reforming into other compounds such CO and CO_2 which is why CO and CO_2 are positive values. This mass balance did not take H_2, CH_4, H_2O nor other heavy hydrocarbons into account which may be up to 30% of the total mass.

4.10 Validation of Results to Other Studies

When a study is performed it must be validated against known sources of data to ensure the quality of the data is high enough. When the CO evolution for corn in this work was compared to the same data in Ulstad's work the results were very similar to the CO sensor. The CO yields for paper sludge in this work are approximately 80% higher

than in Ulstad's work. This may be due to using a large biomass sample mass which increased the exposed surface area. Also, the CO yields in this work are significantly higher than those in works done by DeCristofaro in 2009 as well as in Lenert's work in 2008 which were done at similar operating conditions but both with oat hulls. A comparison between corn and oat hulls is rather difficult to perform but all results are of the same order of magnitude. Both of their works didn't examine O_2 to the degree as was presented in this work. As discussed, excess O_2 enhances gasification so it would be expected that when excess O_2 is present a higher yield of CO would result. DeCristofaro examined excess O_2 in the gasification stream and found that CO yields benefitted from O_2 concentrations of up to 10%. But an optimum level of O_2 was never calculated in his work due to time constraints. This work used a similar method of increasing the oxygen concentration in the gasification stream by adding excess oxygen into the heating torch. It was found that an optimum level of 2-8% oxygen concentration in the gasification stream provided the best CO yields. The CO_2 concentration was highest for paper sludge in the current work which was also found to be true for Ulstad's work.

CHAPTER 5

CONCLUSIONS AND FUTURE WORK

5.1 Conclusions

Biomass gasification is a process through which biomass materials are converted into useful energy through incomplete combustion. This process is difficult to simulate due to the complex chemistry taking place in the drying, pyrolysis, and char gasification zones. These zones overlap and occur simultaneously throughout the gasification process and they vary in size for different types of gasifiers. This work attempts to understand a sub-process of the gasification stage known as pyrolysis. During this stage, the majority of the volatiles stored within the biomass are released when the bonds holding the different molecules break apart in the presence of heat. In an effort to better understand the fundamentals of this process, multiple biomasses (corn kernels, paper sludge, and wood chips), were gasified for up to 220 seconds to complete the pyrolysis stage at temperatures ranging from 400-700°C. From these pyrolysis experiments, the gas evolution of CO, CO_2, H_2, and O_2 was measured with a gas chromatograph at different steps throughout the gasification process. The gas evolution of CO was measured continuously throughout the gasification process by a specific CO sensor and then was compared to the data from the gas chromatograph. These measurements were taken to understand how the different gasses form in relation to each other. This knowledge can be later used in CFD models or in industrial systems.

The gas evolution of CO was measured and it was found that the peak gas evolution increased with an increase in temperature. The data from the CO sensor correlated with the data from the gas chromatograph further increasing the confidence in the accuracy of the measurements. The time to peak CO evolution significantly increased with a decrease in temperature for corn. The time to peak CO evolution for paper sludge and wood chips remained fairly constant at approximately 25-30 seconds but as the temperature increased so did the concentration of CO produced. The greatest amount of

evolved CO was measured for wood chips at 700°C. The greatest amount of evolved CO_2 was measured for paper sludge at 700°C. Pyrolysis occurred slowest for corn kernels than it did for both paper sludge and wood chips. This is believed to be related to the small size and high density of the corn kernels. The relative surface area of the corn kernel exposed to the gasification stream was much smaller than the other biomasses. These three characteristics combined yielded a longer pyrolysis reaction. The total CO production of wood chips was higher at all temperatures in comparison to corn kernels and paper sludge. Corn kernels yielded the second most total CO. Paper sludge produced the least due to its high moisture content which increased the amount of energy required to dry the biomass samples. The particle size of the biomass affects the gasification products as seen from the CO gas evolution comparison for wood chips and corn kernels.

The CO_2 level, as measured by gas chromatography, showed that corn reached its peak CO_2 concentration slower than wood chips and paper sludge. Paper sludge yielded the highest concentration of CO_2, surprisingly. This may be due again to the low density and large exposed surface area of the paper sludge.

A small concentration of additional O_2 was injected through the torch. The amount of O_2 was measured and was found to play a significant role in the production of CO. It was found that when the excess O_2 was increased, larger amounts of O_2 were consumed and larger amounts of CO were produced, at amounts of up to 10% excess O_2. Corn kernels consumed the least O_2 at lower temperatures whereas wood chips and paper sludge consumed the most over the lower temperature ranges. Wood chips consumed the most O_2 in comparison to paper sludge and corn over all temperature ranges. The larger particle size of the wood chips and paper sludge played a significant role in O_2 consumption.

No H_2 or CH_4 was measured due to the short residence time of about 0.2 seconds, as expected. Modern, industrial sized gasifiers with longer residence times will measure

significant volumes of H_2. The lack of CH_4 is due to the reformation of CH_4 into CO and CO_2 in the presence of heat and O_2.

The results of this work are beneficial for CFD modelers because most CFD modelers are lacking this type of pyrolysis data so they can use the inputs provided in this current work to increase the accuracy of their models. This work will also help industrial gasifiers operate with the proper biomass at the optimal temperature level for maximization CO and CO_2 production.

5.2 Future Work

The future of this work depends on changes in the design of the heating system. The dual heating system, an electric heater and an oxy acetylene torch, used in this work enabled high temperature gasification but the torch produced additional H_2O and CO_2. This additional CO_2 was accounted for, and the H_2O mixed with the biomass tars and created additional sensing problems in this experiment. Ideally, the heating system would employ only an electric heater capable of high heating rates and the ability to provide heat at a maximum of 1200°C. An electric heater is desired because it provides heat from electrical resistance and does not produce any permanent gasses such as CO_2 or H_2O. In this work, a larger electric heater was not used due to cost constraints.

A second major change would be in the testing method used. This work used several gas sampling bags to capture the synthesis gas over the pyrolysis period. However, the gas sampling bags time averaged the concentration of each bag because they took ten seconds to fill. Also when the bag was being switched a portion of the synthesis gas was not captured for testing. A system that allows switching of the gas into one bag while the next bag is being prepared to be filled would be useful to ensure that all the gas during pyrolysis is captured. Also, to increase the quality of the data and remove outliers, more biomass samples must be gasified at each operating parameter. To better

detect CO and H_2 with the gas chromatograph, it should be calibrated a standard CO and H_2 calibration gas of less than 1%.

Additional experiments at higher temperatures should be performed to better understand the pyrolysis stage. This work focused on low temperature gasification. Performing experiments at higher temperatures would help to mimic real world operating parameters. Lastly, an attempt to increase the gas and solid residence time would produce more realistic results.

REFERENCES

Bartholomew, C.H., 1982. Carbon deposition in steam reforming and methanation. Catal. Rev. -Sci. Eng. 24, 67.

Chen, G., J. Andries, Z. Luo, H. Spliethoff. “Biomass pyrolysis/gasification for product gas production: the overall investigation of parametric effects.” Energy Conversion and Management 44 (2003) 1875–1884.

DeCristofaro E: Gas Evolution from Biomass Gasification and Pyrolysis. Master’s Thesis. The University of Iowa, 2009

Devi, Lopamudra, K. Ptasinski, Frans J. J. Janssen. “A review of the primary measures for tar elimination in biomass gasification processes.” Biomass and Bioenergy 24 (2003): 125-140

Dordt College. 2010 Senior Design Project.

Dupont, Capucine, Jean-Michel Commandre, Paola Gauthier, Guillaume Boissonnet, Sylvain Salvador, and Daniel Schweich. "Biomass pyrolysis experiments in an analytical entrained flow reactor between 1073 K and 1273 K." Fuel (2007).

Fischer-Tropsch Liquids Facility." National Energy Technology Laboratory, U.S. Department of Energy. April 9, 2007. (Dec. 10, 2010)

Khan, A. A., W. de Jong, P. J. Jansens, H. Spliethoff. “Biomass combustion in fluidized bed boilers: Potential problems and remedies.” Fuel Processing Technology 90 (2009): 21-50

Kirubakaran, V., V. Sivaramakrishnan, R. Nalini, T. Sekar, M. Premalatha, and P. Subramanian. "A review on gasification of biomass." Renewable and Sustainable Energy Reviews (2007).

Knoef, H.A.M. Handbook biomass gasification. BTG biomass technology group, 2005

Kumar A, Jones D D, Hanna M A: Thermochemical Biomass Gasification: A Review of the Current Status of the Technology. Energies 2009, 2 (3), 556-581.

Li, X.T., J.R. Grace, C.J. Lim, A.P. Watkinson, H.P. Chen, J.R. Kim. “Biomass gasification in a circulating fluidized bed.” Biomass and Bioenergy 26 (2004): 171-193

Lee, Dong Ho, Haiping Yang, Rong Yan, and David T. Liang. "Prediction of gaseous products from biomass pyrolysis through combined kinetic and thermodynamic simulations." Fuel 88 (2007): 410-17.

Lenert, Andrej, Andrew Ewald, and Catherine Szulyk. Pyrolysis of Biomass to Produce Alternative Fuels. The University of Iowa. 2008.

Lögdberg, S. Master's thesis, KTH Sweden School of Chemical Science and Engineering, 2007.

Loon, Remko van. "Analysis of Biogas Using the Agilent 490 Micro GC Biogas Analyzer." Agilent Technologies, Inc. 2011.

Lv, P. M., Z. H. Xiong, J. Chang, C. Z. Wu, Y. Chen, J. X. Zhu. "An experimental study on biomass air-steam gasification in a fluidized bed." Bioresour. Technol. 95 (2004): 95-101

The Ohio State University: Seed Treatment. Bulletin

Pengmei Lv, Zhenhong Yuan, Longlong Ma, Chuangzhi Wu, Yong Chen, Jingxu Zhu. "Hydrogen-rich gas production from biomass air and oxygen/steam gasification in a downdraft gasifier." Renewable Energy 32 (2007): 2173-2185

Rapagnà, S., A. Latif. "Steam gasification of almond shells in a fluidised bed reactor: the influence of temperature and particle size on product yield and distribution." Biomass and Bioenergy 12 (1997) 281–288.

Reed, Thomas B., and Siddhartha Gaur. A Survey of Biomass Gasification: Gasifier Projects and Manufacturers Around the World. 2nd ed. 2000.
Sadaka S: Pyrolysis *Sungrant Bioweb*. Sungrant Initive, 15 Nov. 2008. Web.

Sjöström, E. (1993). *Wood Chemistry: Fundamentals and Applications*. Academic Press.

Steen, Eric V., and Michael Claeys. "Fischer-Tropsch Catalysts for the Biomass-to-Liquid Process." Chem. Eng. Technology 31 (2008). 18 July 2008. [58] [4]

Thiessen, Sam. "Ag Bio Power System Capabilities." 20 Aug. 2008. Interview conducted by the Eric DeCristofaro.

Turn, S.; Kinoshita, C.; Zhang, Z.; Ishimura, D.; Zhou, J. An experimental investigation of hydrogen production from biomass gasification. *Int. J. Hydrogen Energy* **1998**, *23*, 641–648.

Ulstad, E. Gas Evolution of Corn Kernels, Oat hulls, and Paper Sludge from Biomass Gasification. Master's Thesis. The University of Iowa, 2010

Van Bibber, Lawrence. "Baseline Technical and Economic Assessment of a Commercial Scale

Wang, Y., K. Yoshikawa, T. Namioka, Y. Hashimoto. "Performance optimization of two-staged gasification system for woody biomass." Fuel Process Technol. 88 (2007): 243-250

Warnecke, Ragner. "Gasification of biomass: comparison of fixed bed and fluidized bed gasifier." Biomass and Bioenergy 18 (2000): 489-497

Williams, Paul, and Serpil Besler. "The influence of temperature and heating rate on the slow pyrolysis of biomass." Renewable Energy 7 (1996): 233-250

Xu, G.,T. Suda, Y. Matsuzawa, H. Tani, T. Fujimori, T. Murakami. "Some process fundamentals of biomass gasification in dual fluidized bed." Fuel 86 (2007) 244–255.

Yamazaki, T., H. Kozu, S. Yamagata, N. Murao, S. Ohta, and others. "T. Effect of superficial velocity on tar from downdraft gasification of biomass." Energy Fuels 19 (2005): 1186-1191